Water Resources Research

Supporting Information for

Are our dynamic water quality models too complex? A comparison of a new parsimonious phosphorus model, SimplyP, and INCA-P

L.A. Jackson-Blake[a,b], J.E. Sample[a,b], A.J. Wade[c], R.C. Helliwell[b], R.A. Skeffington[c]

[a] Norwegian Institute for Water Research (NIVA), Gaustadalleen 21, 0349 Oslo, Norway
[b] The James Hutton Institute, Macaulay Drive, Aberdeen, AB15 8QH, UK
[c] Department of Geography and Environmental Science, University of Reading, RG6 6DW, UK

Contents of this file

Introduction

This supplementary information contains a full description of the SimplyP model, a newly-developed parsimonious catchment-scale dynamic water quality model for simulating hydrology, phosphorus and sediment dynamics in catchments. The model was originally developed in 2015 at the James Hutton Institute (Scotland), as part of L. Jackson-Blake's PhD. In the following document, a full description is provided of model aims, scope and scale, the processes and equations included in SimplyP v1.0 and the underlying scientific rationale, a description of numerical methods used to solve the equations, and a suggestion of model development priorities.

Text S1.

SimplyP v1.0 model description

Contents

1. Introduction

SimplyP is a parsimonious catchment-scale dynamic water quality model, which simulates hydrology, phosphorus (P) and sediment dynamics in catchments. The model was originally developed in 2015 at the James Hutton Institute (Scotland), as part of L. Jackson-Blake's PhD. The model is under development, lead by NIVA (Norway), with input from the James Hutton Institute. Here, we present model aims, scope and scale (Section 3) and give a detailed overview of the processes and equations included in SimplyP v1.0, as well as the underlying scientific rationale. A suggestion of model development priorities is provided in Section 5.

2. Model availability

SimplyP v1.0 model code is open source (https://github.com/LeahJB/SimplyP). Running the model requires a Python installation able to run iPython notebooks (e.g. WinPython; http://winpython.sourceforge.net/); instructions for installing WinPython and running the model using an example dataset are provided in the GitHub repository. Model parameters are input to the model via a simple Excel interface; recommendations for default, minimum and maximum values and potential data sources are provided in Table 11.

3. Model aims, scope and scale

3.1 Model aims

SimplyP aims to be process-based, i.e. model equations reflect hypotheses about the processes governing system behaviour. The aim in developing SimplyP was to minimize the process representation to only those processes that appear to control the catchment response, whilst maintaining the flexibility and functionality required for the model to be useful in hypothesis and scenario testing. The process representation aims to be simple enough to allow parameter values to be constrained using available observational data. What is presented here is a first prototype, the aim being to attempt a proof-of-concept that simple can be as good as complex. The hope is that this simple model could provide a useful benchmark when choosing between different models, or, after further testing, be a useful modelling tool in its own right.

SimplyP was developed with a number of potential uses in mind, including: (1) interpolation of sparse monitoring data, to provide more ecologically-relevant in-stream phosphorus concentrations or more accurate estimates of loads delivered downstream to lakes or estuaries; (2) hypothesis testing and highlighting knowledge and data gaps. This in turn could be used to help design monitoring programmes, highlight experimental needs, and prioritise areas for future model development; (3) exploring the potential response of the system to future change, especially in terms of anticipated storm and low-flow dynamics; and (4) providing evidence to support decision-making, for example to help set water quality and load reduction goals and to advise on the best means of achieving those goals.

A particular requirement at present is for models which can predict time lags in the system due to stores of 'legacy' P, P which has accumulated in the catchment along transport pathways in the land-freshwater continuum. These legacy P stores may become net sources of P if inputs to the store are reduced, potentially confounding management efforts aimed at reducing in-stream P concentrations (Sharpley et al., 2013). Stores of legacy P include: (1) soil P, from historic applications of fertilizer and manure in excess of crop requirements; (2) terrestrial sediment-bound P, stored in areas where local topography promotes sediment deposition; (3) groundwater P, due to percolation of P-rich water from agriculture or sewage; (4) P in up-stream impoundments (e.g. lakes, reservoirs and canals); and (5) P in in-stream bed sediments. The latter may be sourced from the deposition of particulate P in areas of slower flow (e.g. pools, floodplains), or from the adsorption of dissolved P from the water column, particularly downstream of sewage treatment works. The aim here is for the model to reproduce the first of these stores, soil P, as this is often the largest and the most pervasive legacy source of P to the environment (Jarvie et al., 2013a; Kleinman et al., 2011; Sharpley et

al., 2013). The remaining legacy P stores are beyond the scope of this initial version of the model, though recommendations are provided for how more legacy P sources could be incorporated.

In the future, it is likely that well-devised auto-calibration and uncertainty analysis routines will become pre-requisites for model applications. To date, attempts to bring about a shift in modeller behaviour have focused on improving algorithms and making them more available, but have largely over-looked other important barriers such as the subjectivity of the analyses (Jackson-Blake and Starrfelt, 2015) and the often prohibitively large amounts of time required to set up and conduct such analyses. We believe that the use of auto-calibration and uncertainty analysis tools would increase substantially if more attention were paid to: (1) developing models with fewer parameters, so all uncertain parameters can be included in an analysis; (2) reducing the number of interacting parameters, to reduce non-identifiability issues and the need for time-consuming *ad hoc* code to be written; and (3) maximising the number of parameters which can in principle be measured, and therefore given informative priors. SimplyP was developed with these three aims in mind. In practice, the number of parameters that can be calibrated in a given study area depends on data available for model calibration and for constraining model parameters to plausible ranges. However, studies have rarely successfully explored more than 40-dimensional parameter spaces (e.g. Dean et al., 2009; Jackson-Blake and Starrfelt, 2015; Starrfelt and Kaste, 2014), so an upper limit of 40 parameters was decided on.

3.2 Model temporal and spatial scale

The model is dynamic and currently runs at a daily time step, short enough to capture much of the variability in catchment hydrology and the associated delivery of dissolved and particulate matter to the water course, yet not so short that computing run times become prohibitively long when the model is run to explore longer term trends. A daily time step is also compatible with the majority of widely-available meteorological data sets used to drive the model.

The model is spatially semi-distributed, as a compromise between the complexity of fully-distributed methodologies and the lack of spatial process representation in fully lumped models. The catchment is broken down into perceived biophysical regions, thereby allowing a certain amount of the spatial variability in processes and outputs to be simulated, whilst reducing input data requirements and computing run times. The main disadvantage compared to fully-distributed models is that the interconnectedness of different parts of the landscape is not included, but in most areas this is justified by the lack of input data for a finer-scale division of the landscape and the reduced computing run times. The catchment area may be split into:

1. *Sub-catchments and associated reaches*, which should be defined based on the presence of monitoring stations, sewage treatment work inputs, or major changes in terrestrial conditions such as geology, topography or soil type. The model is run for each sub-catchment in turn, and reach outputs are fed sequentially down-stream.

2. *Grouped soil properties and broad land management, termed the land class*. A summary of the land class sub-divisions is given in Table 1. For dissolved P processes, two land classes are considered, a '*high P*' class and a '*low P*' class. Land within a class should have a similar annual P budget, soil P content and hydrological characteristics, or area-weighted properties should be used. A third optional '*newly-converted*' class may also be included, to take into account legacy soil P when land use conversion occurs, or the lack of legacy soil P in new agricultural land. For sediment and particulate P processes, the high P class may be further sub-divided in two to account for differences in erodibility (e.g. agricultural land could be split into improved grassland and arable land). Finally, the proportion of spring versus autumn-sown crops that make up any arable land may be taken into account when calculating the variation in soil erodibility due to plant cover through time.

   In highly agricultural areas where there is no 'low P' land, if the model is to be used to explore impacts of changing fertilizer or manure inputs or land use, the expected inactive P content for semi-

natural land in the area must still be provided, to provide a reference point for the P enrichment of agricultural soils, but the 'low P' class coverage of the catchment would be set to zero.

<table>
<tr><th>Processes</th><th colspan="3">Landscape division</th></tr>
<tr><td>Dissolved P</td><td colspan="2">High P
e.g. arable land, improved grassland</td><td>Low P
e.g. unfertilized forest, moorland, rough grassland</td></tr>
<tr><td rowspan="3">Sediment & particulate P</td><td colspan="2">High P</td><td rowspan="3">Low P</td></tr>
<tr><td colspan="2">High erodibility*
e.g. arable</td><td rowspan="2">Low erodibility*
e.g. improved grassland</td></tr>
<tr><td>Spring-sown*</td><td>Winter-sown*</td></tr>
</table>

*Table 1: Land class sub-divisions available for use in SimplyP. These differ according to the process being simulated (dissolved or particulate phosphorus processes). *Optional*

4. SimplyP model structure and equations

A summary of the main stores and fluxes of water, sediment and P is provided in Figure 1. The model includes the following components:

- A snow accumulation and melt model (Section 4.1.1)
- Rainfall-runoff (Section 4.1.2) and in-stream hydrology (Section 4.1.3)
- Sediment delivery to the watercourse and in-stream transport (Section 4.2)
- Terrestrial and in-stream P processes (Section 0)

Dissolved and particulate P are simulated separately as total dissolved P (TDP) and particulate P (PP). PP is assumed to be sediment-bound and no distinction is made between organic and mineral P.

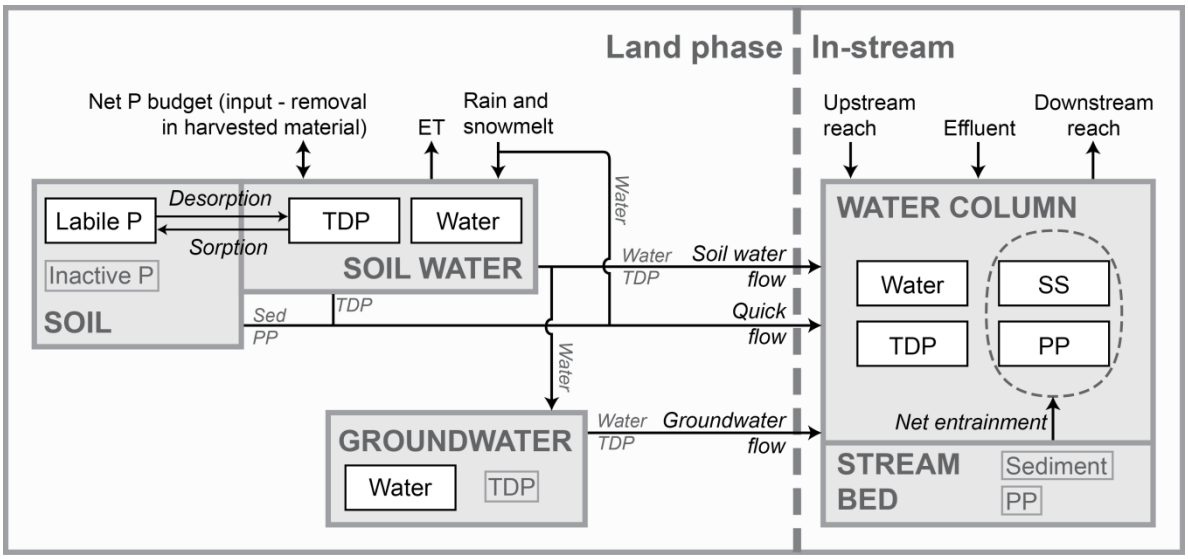

Figure 1: Schematic of the main stores, processes and pathways included in the model. White boxes show the state variables whose volume (water) or mass (sediment, P species) is tracked. Arrows show fluxes within and between compartments. P: phosphorus, SS: suspended sediment, TDP: total dissolved P, PP: particulate P, ET: evapotranspiration.

4.1 Hydrology

4.1.1 Hydrological inputs

Input time series of precipitation and potential evapotranspiration (PET) are required. If the snow module is not used, then these are used to drive hydrological processes in the model. If the snow accumulation and melt

module is used, then air temperature must also be supplied, and a time series of rain plus snowmelt is calculated and used to drive hydrological processes in the model. Parameters and variables used in the hydrological input equations are defined in Table 2.

Variable	Description	Units	Source
D_{snow}	Snowpack depth	mm	Equation 3
$D_{snow,0}$	Initial snowpack depth	mm	Input parameter
f_{DDSM}	Degree-day factor for snowmelt	mm/degree-day °C	Input parameter
P	Hydrological input to the model	mm day^{-1}	Equation 4
$P_{melt,max}$	Potential maximum snowmelt	mm day^{-1}	Equation 2
P_{rain}	Precipitation as rain	mm day^{-1}	Equation 1
P_{snow}	Precipitation as snow	mm day^{-1}	Equation 1
P_{total}	Total precipitation	mm day^{-1}	Input time series
T_{air}	Mean daily air temperature	°C	Input time series

Table 2: Parameters and variables used in calculating hydrological inputs to the model

Within the snow model, precipitation falls as snow when the mean daily air temperature is below 0°C (Equation 1). Potential daily snow melt is calculated using a simple degree-day factor method (USDA, 2004), assuming that melting begins once the air temperature rises above 0°C (Equation 2). Both temperature thresholds are hard-coded into the model at present, but could be readily converted to user-supplied parameters. The degree-day approach to simulating snow melt is one of the simplest formulations. Key limitations are discussed in USDA (2004), in particular: (1) the degree-day factor is assumed to be constant, whilst in reality it varies seasonally and by location; (2) snow melt is only controlled by temperature, and therefore ignores important factors such as snow density; and (3) it is not valid for rain-on-snow events.

Equation 1: Partitioning of total precipitation into rain, P_{rain}, and snow, P_{snow} (mm day^{-1})

When $T_{air} > 0$: $P_{rain} = P_{total}, P_{snow} = 0$
Otherwise: $P_{rain} = 0, P_{snow} = P_{total}$

Equation 2: Potential daily snowmelt, $P_{melt,max}$ (mm day^{-1})

When $T_{air} > 0$: $P_{melt,\,max} = f_{\mathrm{DDSM}}(T_{air} - 0)$

Snow pack depth is then calculated as initial depth plus the change due to snowfall and snowmelt, with the latter limited by the snow pack depth (Equation 3). As snowfall and melt are constant over a day, there is no need for Equation 3 to be formulated as a differential equation. Finally, the sum of rain and snowmelt is used as input to the hydrology model (Equation 4).

Equation 3: Snow pack depth, D_{snow} (mm), where superscript *t* denotes the current time step, and *t-1* the previous time step. This calculation requires a user-supplied initial snowpack depth, $D_{snow,0}$

$$D_{snow}^{t} = D_{snow}^{t-1} + P_{snow}^{t} - \mathrm{minimum}(P_{melt,max}^{t}, D_{snow}^{t-1})$$

Equation 4: Hydrological inputs to the model, P (mm day^{-1})

$$P = P_{rain} + P_{melt}$$

An example of output from the snow module for the Tarland Burn catchment for the period 2004-2005 is shown in Figure 2.

The snow model uses mean daily air temperature as input, which could lead to under- or over-estimation of snowfall and snowmelt. In areas where there is significant winter accumulation of snow, a possible future modification to the model would be to use a more sophisticated representation of temperature variation throughout a day, for example using a triangular or a sinusoidal shape.

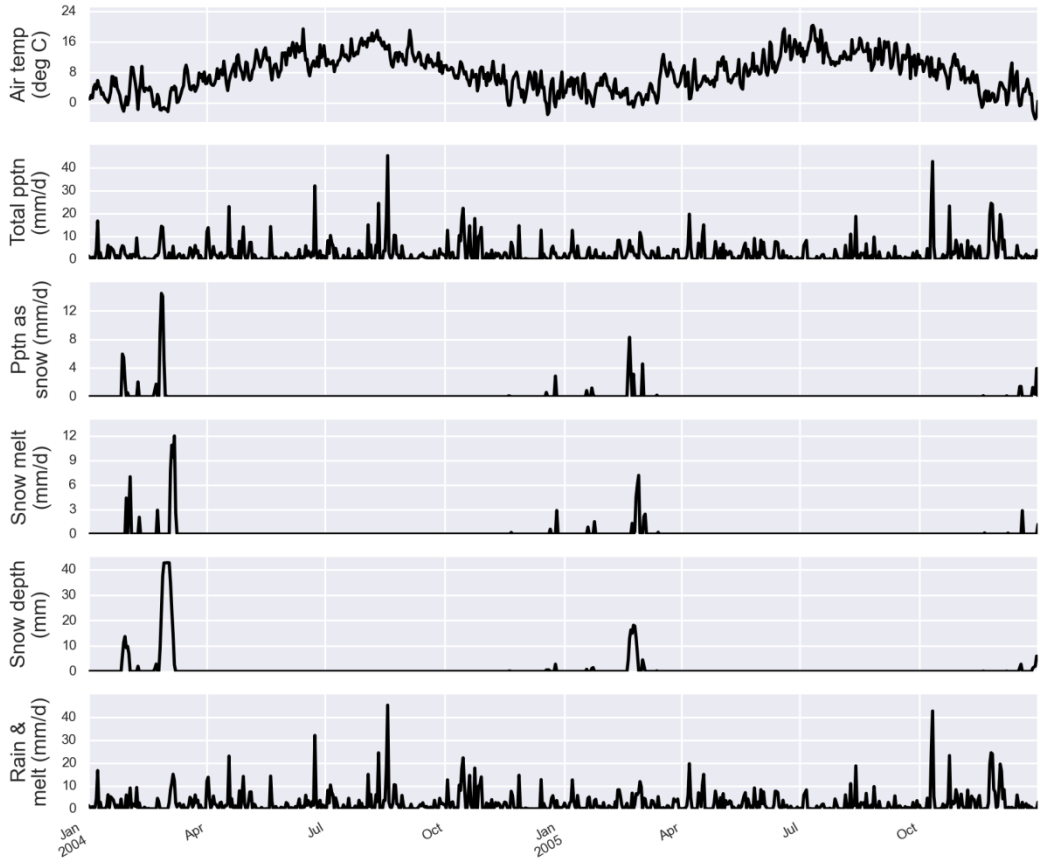

Figure 2: Inputs to and outputs from the snow accumulation and melt module, using input data for the Tarland Burn catchment. 'Pptn' is precipitation. Snow depths are given as mm of water equivalent.

4.1.2 Terrestrial hydrology

A hydrology model provides the foundation for any water quality model, as the flow of water transports matter from the land to the stream. To simulate hydrology alone, simple models may be appropriate, with just a couple of calibration parameters (e.g. IHACRES, Croke et al., 2006). However, to be able to simulate the transport of both dissolved and particulate P under varying flow conditions, a slightly more complex representation of terrestrial hydrology is needed. Here, three terrestrial flow paths are taken into account: (1) quick flow, to simulate water, sediment and P inputs to the watercourse during larger rainfall events and when soils are dry (and therefore little soil water flow occurs); (2) soil water flow, responsible for TDP leaching from soils and groundwater recharge, and (3) groundwater flow, which is important for baseflow P concentrations.

The soil water and groundwater equations used were based on those described by Sample (2015), who provides a full description of their derivation (last accessed March 2016). For convenience, volumes and fluxes are expressed as water depths per unit area in units of mm or mm day^{-1}. Associated real volumes can be derived by multiplying by the catchment area, A_{SC} (km^2), with unit conversions: 1 m^3 = 10^3 A_{SC} mm. Parameters and variables used in the terrestrial hydrology equations are defined in Table 3.

Variable	Description	Units	Source
α	Potential evapotranspiration correction factor	none	Input parameter
β	Base flow index	none	Input parameter
dQ_g/dt	Change in groundwater flow with time	mm day^{-1} day^{-1}	Equation 13
dQ_s/dt	Change in soil water flow with time	mm day^{-1} day^{-1}	Equation 10
dQ_s/dV_s	Change in soil water flow with soil water volume	mm day^{-1} mm^{-1}	Equation 9
dV_g/dt	Change in groundwater volume with time	mm day^{-1}	Equation 11
dV_s/dt	Change in soil water volume with time	mm day^{-1}	Equation 6
E_a	Actual evapotranspiration	mm day^{-1}	Equation 7
E_p	Potential evapotranspiration	mm day^{-1}	Input time series
$f_E(V_s)$	Function to limit evapotranspiration when soil water level drops below field capacity	none	Equation 7
f_{quick}	Proportion of hydrological inputs to the soil that contribute to quick flow	none	Input parameter
$f_{sw}(V_s)$	Function to limit soil water flow once soil water level reaches field capacity	none	Equation 8
P	Hydrological inputs to the soil (rain plus snowmelt)	mm day^{-1}	Equation 4
Q_g	Groundwater flow	mm day^{-1}	Equation 13
$Q_{g,min}$	Minimum groundwater flow	mm day^{-1}	Input parameter
Q_q	Quick flow	mm day^{-1}	Equation 5
Q_s	Soil water flow	mm day^{-1}	Equation 10
T_g	Baseflow recession constant	days	Input parameter
T_s	Soil water time constant	days	Input parameter
V_g	Groundwater volume	mm	Equation 11
V_{FC}	Field capacity	mm m^{-1}	Input parameter
V_s	Soil water volume	mm	Equation 6

Table 3: Parameters and variables used in the terrestrial hydrology equations

a) Quick flow

Quick flow is conceptualised to include a host of rapid flow pathways, including infiltration and saturation excess overland flow, tile drainage, runoff from impervious surfaces and macropore or preferential flow through soils. In practice, it is difficult to differentiate between these various rapid flow paths when calibrating using in-stream discharge data. Therefore as a starting point all were lumped into a single input to the stream, calculated as a function of incoming precipitation. A number of options for characterising quick flow were considered (in order of increasing complexity):

1. Assume quick flow is directly proportional to incoming precipitation and is routed instantaneously to the stream. This involves just one calibration parameter, f_{quick}, the proportion of precipitation that contributes to quick flow:

$$Q_q = f_{quick}P$$

2. Assume quick flow only occurs above some precipitation threshold, I_{max}, with all precipitation routed instantaneously to the stream above this threshold. As with option (1), this involves just one calibration parameter:

$$Q_q = \max\{(P - I_{max}), 0\}$$

3. A third option builds on option 2, including a factor to describe the proportion of the precipitation that contributes to quick flow once the threshold has been exceeded. It therefore has two parameters, f_{quick} and I_{max}:

$$Q_q = f_{quick} \max\{(P - I_{max}),0\}$$

4. Adopt one of the above approaches to describe the hydrological inputs to a quick store of water, and track the change in volume and flow of water in the store. This involves an additional user-input parameter, the time constant of the store, and therefore involves two or three user-supplied parameters. This approach is used by many process-based catchment water quality models, e.g. INCA.

Option 4 was discounted as being unnecessarily complex: the time constant is likely to be set to a small value in most catchments, and so the assumption in options 1 to 3 of quick flow directly entering the stream without a time lag is usually justifiable. As a starting point option 1 was chosen, being the simplest (Equation 5), but future work comparing options within a formal statistical framework would be useful.

Equation 5: Quick flow inputs to the stream, Q_q (mm day^{-1})

$$Q_q = f_{quick}P$$

Despite being simple, this approach allows summer flow events to be simulated, as a proportion of all precipitation enters the stream even when soil water level is below field capacity (often the case during the summer in temperate regions), when no soil water flow is simulated. It is important to be able to simulate these summer flow events, as they are often associated with nutrient peaks. Several models address the problem by adding in an additional quick flow path when soil water drops below field capacity (e.g. PERSiST, Futter et al., 2014). However, it is conceptually more consistent for this process to occur whatever the soil water level, as in Equation 5.

An important limitation of the adopted approach is a lack of seasonality in the generation of quick flow; in reality, quick flow is likely to be higher when soils are saturated, which is often the case during winter in temperate regions. A potential future extension to the model would be to include this saturation excess flow, which would require a re-formulation of the soil water equations.

b) Soil water

The soil water ordinary differential equations (ODEs) are solved separately for semi-natural and agricultural land, so the equations described in this section are present in the model for both land use classes. The change in soil water volume with time is given by Equation 6. Inputs to the soil water are from rainfall and snowmelt (Section 4.1.1), taking into account the proportion that is routed to quick flow; outputs are through evapotranspiration (E_a) and soil water flow.

Equation 6: Rate of change in soil water volume, V_s, with respect to time (mm day^{-1})

$$\frac{dV_s}{dt} = (1 - f_{quick})P - E_a - Q_s$$

E_a is calculated from a user-supplied time series of potential evapotranspiration (E_P), taking into account: (1) differences between land cover and topography in the study catchment compared to reference values used to compute E_p, through the optional use of a correction factor, and (2) moisture limitation once soil water drops below field capacity (Equation 7). To achieve the link between evapotranspiration and soil water content, an additional variable is needed in Equation 7 which tends to 1 as V_s approaches field capacity and to 0 as V_s tends to 0. A convenient function which displays this behaviour is $f_E(V_s) = 1\text{-}e^{\mu V_s}$, where μ is a tuning parameter that determines the shape of the curve (Fenicia et al., 2011). The value of μ is determined within the model as a function of field capacity: for the desired behaviour, E_A should be close to E_P when the soil water is at field capacity, i.e:

$$E_P = k\,E_A \text{ when } V_s = V_{FC}, \text{ where } k \text{ is near 1}$$

Substituting this into Equation 7 and re-arranging gives $\mu = -\ln(1\text{-}k)/V_{FC}$. The $f_E(V_s)$ function is plotted in Figure 3 for a variety of values of k and for the minimum and maximum likely field capacity values (100 to 450 mm/m; Ratliff et al., 1983). Based on this plot, k was fixed at 0.99 so that $f_E(V_s)$ is close to 1 at field capacity and drops away relatively quickly below field capacity.

Equation 7: Actual evapotranspiration, E_a (mm day^{-1}). The function $f_E(V_s)$ limits evapotranspiration when soil water content drops below field capacity

$$E_a = \alpha E_p \, f_E(V_s) = \alpha E_p \, (1 - e^{-\mu V_s}), \text{where } \mu = \frac{-\ln(0.01)}{V_{FC}}$$

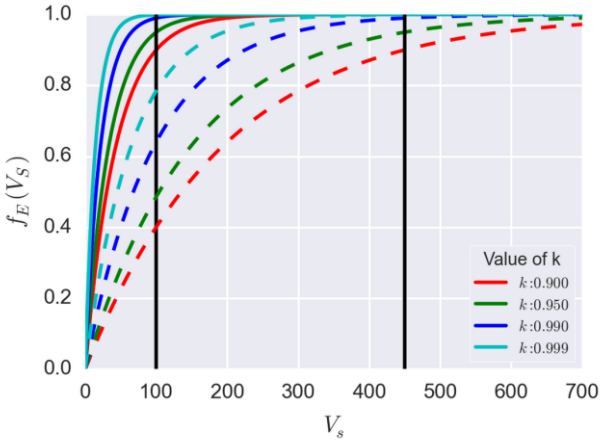

Figure 3: Relationship between $f_E(V_s)$ and soil water volume (V_s/mm) for a variety of k factors, where $f_E(V_s) = 1\text{-}e^{\mu V_s}$ and $\mu = \text{-}ln(k)/V_{FC}$. The vertical lines mark the minimum and maximum likely values for field capacity (FC). Solid lines: FC=100; dashed lines: FC=450 mm m^{-1}.

It is assumed that soil water flow only takes place when the soil water level is above field capacity and that flow is proportional to the volume of water above field capacity (Equation 8). The constant of proportionality is $1/T_s$, where T_s is the soil water time constant. The additional function in Equation 8, $f_{sw}(V_s)$, prevents soil water flow from occurring when soil water content drops below field capacity. One option is for this function to involve a set of logical conditions (e.g. $f_{sw}(V_s) = 0$ when $V_s > V_{FC}$; otherwise $f_{sw}(V_s) = 1$). However, this kind of logic introduces non-differentiable discontinuities into the ODE. Instead, a continuous sigmoid function was used (Fenicia et al., 2011), which yields a curve which switches rapidly from zero to one around field capacity (Figure 4).

Equation 8: Discharge from the soil water store, Q_s (mm day^{-1})

$$Q_s = \frac{1}{T_s}(V_s - V_{FC}) \, f_{sw}(V_s) = \frac{1}{T_s}(V_s - V_{FC}) \left(\frac{1}{1 + e^{(V_{FC} - V_s)}} \right)$$

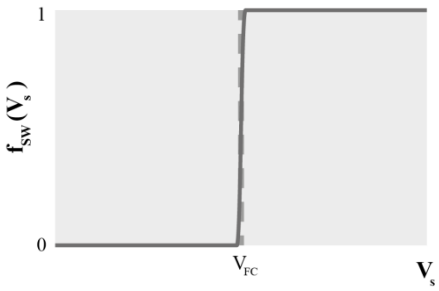

Figure 4: Schematic demonstrating the form $f_{sw}(V_s)$ takes when a sigmoid curve is used

To derive an equation for the rate of change in soil water flow with time, dQ_s/dt, Equation 8 must be differentiated with respect to time. To do this, dQ_s/dV_s is first defined by differentiating Equation 8 with respect to soil water volume (Equation 9), which is then used to derive dQ_s/dt (Equation 10).

Equation 9: Rate of change in soil water flow, Q_s, with respect to soil water volume (day^{-1})

$$\frac{dQ_s}{dV_s} = \frac{(V_s - V_{FC})e^{V_{FC} - V_s}}{T_s(e^{V_{FC} - V_s} + 1)^2} + \frac{1}{T_s(e^{V_{FC} - V_s} + 1)}$$

Equation 10: Rate of change in soil water flow, Q_s, with respect to time (mm day^{-2})

$$\frac{dQ_s}{dt} = \frac{dV_s}{dt}\frac{dQ_s}{dV_s}$$

Finally, a proportion (β) of the discharge from the soil box is assumed to percolate to groundwater, whilst the remainder of the soil water flow ($1 - \beta Q_s$) is assumed to travel to the stream along shallow flow pathways.

c) Groundwater

The rate of change of groundwater volume with time is controlled by the balance of inputs from the soil water and outputs via groundwater flow (Equation 11). Percolation from the soil water is calculated as a fraction (β) of the soil water outflow (where β is the baseflow index). Groundwater flow is assumed to be directly proportional to groundwater volume (Equation 12), and can be differentiated with respect to V_g to give $1/T_g$, where T_g is the baseflow recession constant. As with the soil water flow, the rate of change in groundwater flow with time is then calculated as the product of dV_g/dt and dQ_g/dV_g (Equation 13). The baseflow recession constant is determined through model calibration or from discharge observations using hydrograph separation techniques (e.g. Van Dijk, 2010). Beck et al. (2013) have produced a global dataset of baseflow index and recession constants which could provide useful starting points for model calibration.

Equation 11: Rate of change of groundwater volume, V_g, with time (mm day^{-1})

$$\frac{dV_g}{dt} = \beta Q_s - Q_g$$

Equation 12: Relationship between groundwater flow and volume

$$Q_g = \frac{1}{T_g}V_g; \text{therefore} \frac{dQ_g}{dV_g} = \frac{1}{T_g}$$

Equation 13: Rate of change of groundwater flow, Q_g, with time (mm day^{-1} day^{-1})

$$\frac{dQ_g}{dt} = \frac{dV_g}{dt}\frac{dQ_g}{dV_g} = \frac{\beta Q_s - Q_g}{T_g}, \text{where } Q_g = \text{maximum}(Q_{g,min}, Q_g)$$

The minimum groundwater flow parameter in Equation 13, $Q_{g,min}$, prevents groundwater flow from dropping below a user-specified threshold. Without this, sustained periods when soil water is below field capacity may result in little groundwater recharge and under-simulation of low flows (red line in Figure 5 for the Tarland catchment). This threshold is implemented by testing whether the groundwater flow at the end of the day is below the user-specified threshold. If it is, the initial conditions at the start of the next time step are set to the threshold. It is therefore possible for groundwater flow within a day to drop below the threshold, but generally not by much.

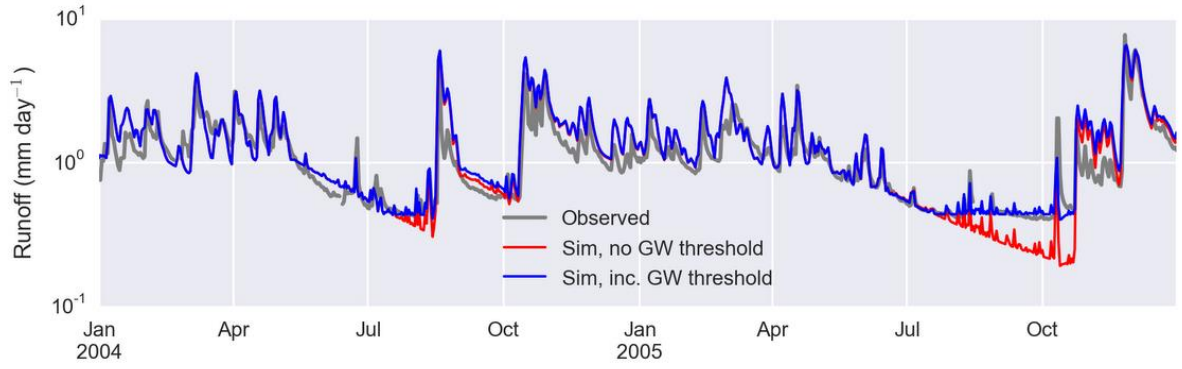

Figure 5: Comparison of simulated runoff with and without inclusion of a minimum groundwater flow in the Tarland catchment. Note log scale.

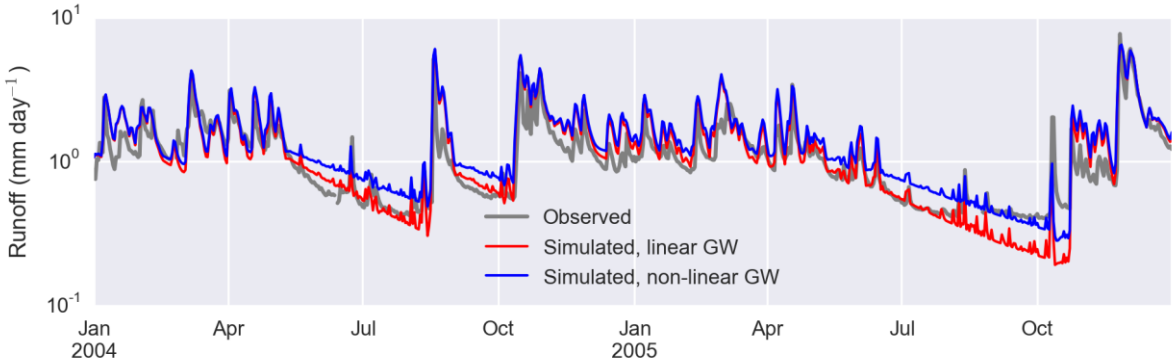

Figure 6: Comparison of simulated runoff generated using a linear and a non-linear groundwater reservoir in the Tarland. Note the log scale.

Poor representation of low flows is a common weakness in hydrological simulations (Fenicia et al., 2006), leading to potentially large errors in simulated solute concentrations during the ecologically-sensitive summer period. Whilst preventing groundwater flow from dropping below a certain threshold improves the simulation, it is not an ideal solution: (1) it circumvents the fact that something is wrong with the model conceptualisation if sustained summer baseflows cannot be simulated, and (2) it does not satisfy the internal catchment water balance, as the excess water required to sustain groundwater at the user-specified threshold is not sourced from within the catchment. This approach therefore works for the purposes of developing a prototype model, and indeed is that adopted by e.g. INCA. However, alternative options were also considered, and should be a priority for future development of the model. These include:

1) Replacing the linear relationship between groundwater volume and flow with a non-linear relationship, so that $V_g = T_g Q^k$, as described by Wittenberg (1999), where k, the non-linear coefficient, reflects the influence of aquifer properties on Q_g. Equations for the rates of change in groundwater volume and flow therefore become:

$$\frac{dQ_g}{dV_g} = \frac{V_g^{\frac{1-k}{k}}}{kT_g^{\frac{1}{k}}} \text{ (which simplifies to } \frac{1}{\mathrm{T_g}} \text{ when k = 1)}$$

$$\frac{dV_g}{dt} = \beta Q_s - \left(\frac{V_g}{T_g}\right)^{\frac{1}{k}}$$

$$\frac{dQ_g}{dt} = \frac{dQ_g}{dV_g}\frac{dV_g}{dt}$$

A comparison of simulations using a linear and a non-linear groundwater store in the Tarland are shown in Figure 6. In this case the non-linear model produces a flatter recession, but simulated low flows are

too high. Discussions as to whether the groundwater storage-discharge relationship should be considered linear or non-linear have been on-going in the literature for some time, and certainly in some cases a non-linear reservoir appears to perform better (e.g. Gan and Luo, 2013). Other researchers have added in additional storage boxes to help improve model performance (e.g. Luo et al., 2012). In cases this may be justified, but Fenicia et al. (2006) make a strong argument for non-linear reservoirs often appearing to perform better only when important fluxes into or out of the groundwater storage zone have been neglected.

2) The second option considered was therefore that the model is missing an additional flux into the groundwater, e.g. slow recharge from the unsaturated zone. Possible alternative formulations of the soil water store, which would allow for some groundwater recharge to occur when the soil water level drops below field capacity, include:

    a. Adding in a small, constant flux from the soil water box to the groundwater, which is independent of soil water content. This would require a user-calibrated parameter to set the flux, and a function as used in Equation 7 to prevent negative soil water volumes.

    b. Changing the shape of the sigmoid function used to limit soil water drainage below field capacity, so that it behaves less like a step function and allows some continued percolation to groundwater below field capacity. This is a mechanistically justifiable option, as soils continue to produce water when water contents drop below field capacity, although the fluxes involved vary with soil type and texture (Twarakavi et al., 2009). Some practicalities of this option would need careful consideration, e.g. choosing an appropriate shape parameter for all possible values of field capacity, to ensure zero flow when water level drops to zero.

        The model only considers average conditions over the catchment, whilst in reality, although catchment-average soil water content may be at or below field capacity, soils in parts of the catchment (e.g. at the foot of slopes or in hollows) are likely to remain above field capacity, and therefore able to feed water into groundwater and surface watercourses. This is a limitation of using a semi-distributed approach, and provides further justification for using a less steep sigmoid function.

In summary, the simple linear store with a user-supplied minimum groundwater flow provides a working solution to the problem of simulating summer low flows, and is suitable for the purposes of the prototype model being developed here. However, improved realism should be achievable without much increase in model complexity, and exploring options to achieve this should be a high priority for any future development efforts.

d) Example model output

An example of terrestrial hydrology output for the Tarland Burn catchment for the period 2004-2005 is shown in Figure 7, using time constants of 1 day for agricultural land and 10 days for semi-natural land. For both land use classes, soil water volume is at or above field capacity for most of the winter and then drops below field capacity during the summer, when quick flow provides the only soil input to the stream. The larger soil water time constant in semi-natural land means that it responds more slowly to changing inputs than agricultural soil water, with lower, broader peaks in flow and volume after rainfall. The groundwater time constant is much longer than the soil water time constants (65 days), so changes in groundwater flow and volume are a highly damped version of the changes in the soil water stores.

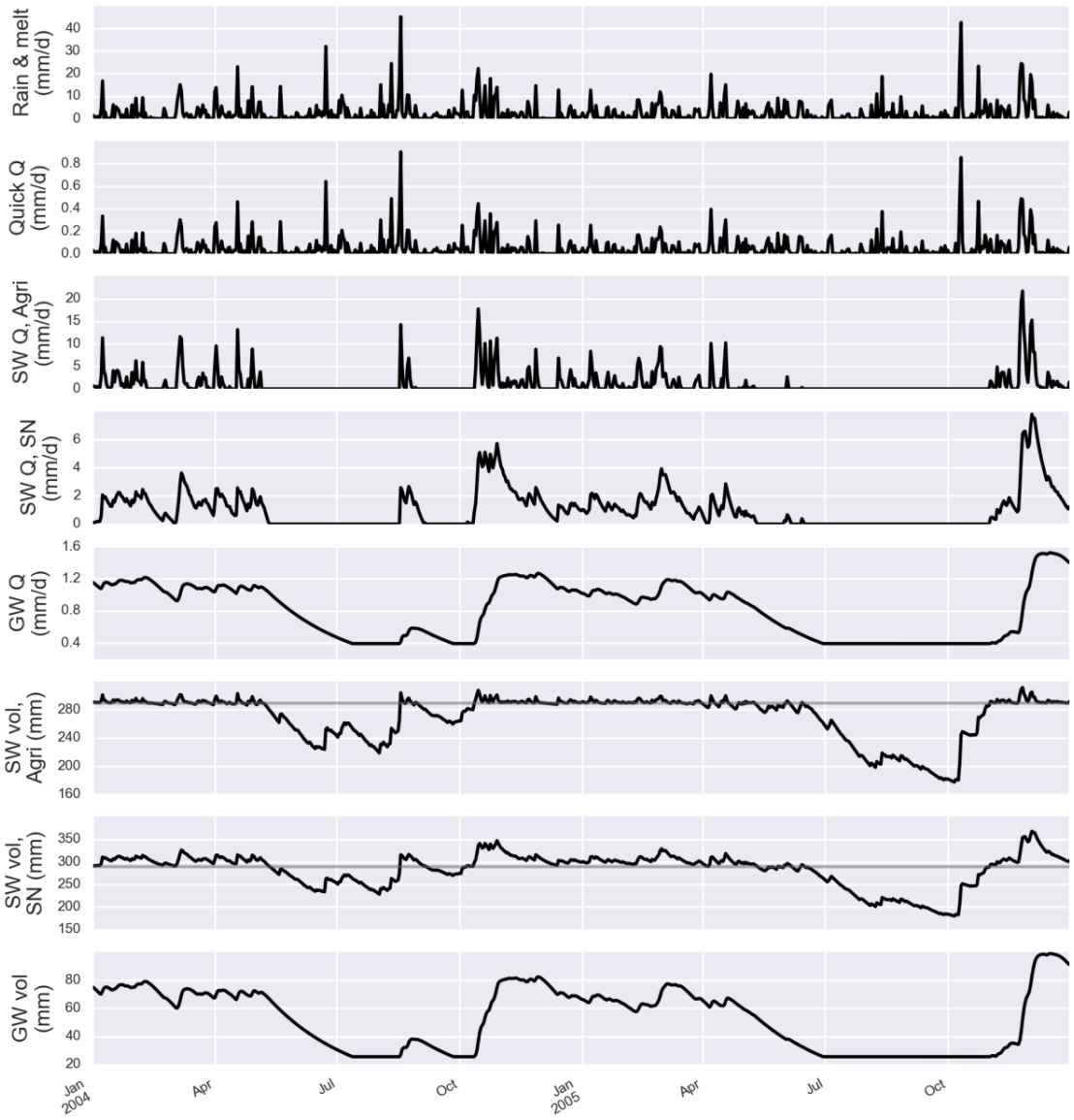

Figure 7: Terrestrial compartment hydrology results in the Tarland catchment. Q: discharge, Vol: volume, SW: soil water, GW: groundwater, Agri: agricultural land, SN: semi-natural land. Grey lines on the soil water volume plots mark the field capacity. N.B. volumes and fluxes are per unit area.

4.1.3 In-stream hydrology

Observed discharge can often be simulated without accounting for within-reach water travel times. However, the water quality model requires estimates of reach volume and discharge, to allow concentrations and fluxes from the reach to be calculated. Parameters and variables used in the instream hydrological equations are defined in Table 4. Note that, as in the terrestrial compartment, all volumes and fluxes are calculated using units of depth per unit area. The simulated daily mean flow is then converted to cumecs for comparison with observations (1 $m^3 s^{-1} = 10^3\ 86400^{-1}\ A_{SC}$ mm day^{-1}, where A_{SC} is sub-catchment area in km^2).

Variable	Description	Units	Source
a	Gradient of in-stream velocity-discharge relationship	m^{-2}	Input parameter
b	Exponent of in-stream velocity-discharge relationship	None	Constant (0.42)
β	Base flow index	None	Input parameter
dQ_r/dt	Rate of change in reach discharge with time	mm day^{-1} day^{-1}	Equation 17
$dQ_{r,av}/dt$	Rate of change in daily mean flow with time	mm day^{-1} day^{-1}	Equation 18
dV_r/dt	Rate of change in reach water volume with time	mm day^{-1} day^{-1}	Equation 14
f_A	Proportion of agricultural land in the sub-catchment	None	Input parameters (f_{Ar} + f_{IG})
f_S	Proportion of semi-natural in the sub-catchment	None	Input parameter
L_{reach}	Reach length	M	Input parameter
Q_g	Groundwater flow	mm day^{-1}	Equation 13
Q_q	Quick flow	mm day^{-1}	Equation 5
Q_s^A	Soil water inputs from agricultural land	mm day^{-1}	Equation 10
Q_s^S	Soil water inputs from semi-natural land	mm day^{-1}	Equation 10
Q_r	Outflow from the reach	mm day^{-1}	Equation 17
$Q_{r,av}$	Daily mean flow from the reach	mm day^{-1}	Equation 18
$Q_{r,US}$	Inputs to the reach from upstream reaches	mm day^{-1}	Model calculates
T_r	Reach time constant	Days	Equation 16
V_r	Reach water volume	Mm	Equation 14

Table 4: Parameters and variables used in the instream hydrology equations

The instream hydrology equations used are similar to those used in other water quality models. The change in water volume in each reach is assumed to be proportional to the difference between input and output fluxes (Equation 14). Input fluxes are from quick flow, soil water flow, groundwater flow and inflow from upstream reaches, and water leaves via the reach outflow. The soil water input to the reach is calculated as the sum of inputs from semi-natural and agricultural land in the catchment.

Equation 14: Rate of change in reach volume, V_r, with time (mm day^{-1})

$$\frac{dV_r}{dt} = Q_q + (1-\beta)(f_A Q_s^A + f_S Q_s^S) + Q_g + Q_{r,US} - Q_r$$

Flow downstream, Q_r, is assumed to be proportional to the reach volume (Equation 15), with a constant of proportionality $1/T_r$ (where T_r is the reach time constant in days). T_r is not however constant as it is in the terrestrial stores, but is inversely proportional to water velocity to account for the shorter residence time of faster flowing water (Equation 16). Water velocity is estimated using an empirical relationship with discharge (Equation 16) (Chapter 14, Chapra, 2008; Leopold and Maddock Jr, 1953), where a is a user-supplied parameter, derived where possible from velocity profiling carried out as part of flow gauging, and b is a non-linear coefficient. The a parameter is the most site-specific, whilst b is usually between 0.3 and 0.5. To reduce model complexity and interactions between these two parameters, the value of b was therefore set as a constant with a value of 0.42, corresponding to the average from over 200 river cross sections in the US and Europe (Wolman et al., 1964). The units of a (m^{-2}) assume that observed velocity and discharge have units of m s^{-1} and m^3 s^{-1}, respectively.

Equation 15: Relationship between reach discharge, Q_r (mm day^{-1}) and volume, V_r (mm)

$$V_r = T_r Q_r = \frac{L_{reach}}{86400\ a} Q_r^{(1-b)}$$

Equation 16: Reach time constant, T_r (days), where U is the water velocity (m s^{-1})

$$T_r = \frac{L_{reach}}{U}; U = aQ_r^b, \text{ so } T_r = \frac{L_{reach}}{86400\ aQ_r^b}$$

The rate of change in discharge with time is given by Equation 17. The time-varying nature of T_r gives rise to the (1-b) factor in the denominator. To get a time series of daily mean flow, the rate of change in discharge with time is integrated with initial conditions set to zero at the start of each day (Equation 18), to provide the

total flux of water leaving the reach over a day. The units of this daily mean flow time series are then converted to cumecs for comparison with observations.

Equation 17: The rate of change in reach discharge, Q_r, with time (mm day^{-1} day^{-1})

$$\frac{dQ_r}{dt} = \frac{1}{T_r(1-b)}\left(Q_q + (1-\beta)(f_A Q_s^A + f_S Q_s^S) + Q_g + Q_{r,US} - Q_r\right)$$

Equation 18: Change in daily mean flow, $Q_{r,av}$ (mm day^{-1}), with time

$$\frac{dQ_{r,av}}{dt} = Q_r$$

The daily mean flow is used to determine the flux from the up-stream reach, $Q_{r,US}$. For the top reach, this is set to zero. For all other reaches, it is set equal to the daily mean flow from the upstream reach for the same time step. In this sense, the reaches are not fully coupled, as simulated within-day changes in flow are not cascaded from reach to reach. However, this assumption simplifies the coding considerably and should be appropriate in all but large, highly flashy systems.

4.2 Sediment processes

4.2.1 In-stream suspended sediment

In-stream SS concentrations are highly variable spatially and temporally, changing in response to terrestrial delivery, stream bank erosion, entrainment of bed sediment material and sediment deposition on floodplains and the stream bed. Terrestrial delivery is in turn controlled by the detachment of soil particles by raindrop impact, flow erosion and transport through the catchment, with deposition in areas of lower water velocity. Important factors affecting in-stream processes include stream power, particle size and type, stream bed morphology, macrophyte cover and antecedent conditions (Merritt et al., 2003). Incorporating these processes into a model would require many parameters to be calibrated, even with a simple formulation. In intensively-studied catchments some terrestrial data may be available to help constrain parameter values, but in most areas calibration is done using only in-stream SS concentration time series, and it is doubtful that these time series contain enough information for such a level of process representation.

Despite the varied and complex processes which represent sediment fluxes to and within streams, in-stream SS concentration has long been known to be well-explained by a simple power law with in-stream discharge: $SS = aQ_r^b$, where SS is suspended sediment concentration, Q_r is in-stream discharge, and a and b are parameters determined by regression (Colby, 1956). There are therefore strong indications that, at the catchment scale, this complexity may be simplified to a remarkably straightforward relationship. Here, this simple power law is therefore taken as the basis for simulating the change in SS mass with time in each stream reach. Parameters and variables used in the sediment equations are defined in Table 5.

Variable	Description	Units	Source
A_{SC}	Sub-catchment area	km^2	Input parameter
C_{cover}	Erosion soil cover factor	none	Equation 26
$C_{measures}$	Erosion management factor	none	Input parameter
dM_{sus}/dt	Rate of change in reach suspended sediment mass with time	kg day^{-1}	Equation 19
$dM_{sus,tot}/dt$	Change in total daily flux of sediment from the stream reach	kg day^{-1}	Equation 23
E_M	Sediment input scaling factor	kg mm^{-1}	Input parameter
E_{sus}	Sediment-discharge rating coefficient	kg mm^{-1}	Equation 21
f_{Ar}	Fraction of arable land in the sub-catchment	none	Input parameter
f_{IG}	Fraction of improved grassland in the sub-catchment	none	Input parameter
f_S	Fraction of semi-natural land in the sub-catchment	none	Input parameter
k_M	Instream erosion and entrainment non-linear coefficient	none	Input parameter
M_{input}	Flux of sediment to the reach from terrestrial and instream sources	kg day^{-1}	Equation 20
M_{sus}	Reach suspended sediment mass	kg	Equation 19
$M_{sus,DS}$	Flux of sediment downstream out of the reach	kg day^{-1}	Equation 22
$M_{sus,US}$	Flux of sediment from upstream reaches	kg day^{-1}	Model calculates
$M_{sus,tot}$	Total daily flux of sediment from the stream reach	kg day^{-1}	Equation 23
Q_r	Reach discharge	mm day^{-1}	Equation 17
$Q_{r,av}$	Daily mean discharge	mm day^{-1}	Equation 18
S_{SC}	Sub-catchment slope	°	Input parameter
S_{reach}	Reach slope	°	Input parameter
SS_r	Mean daily concentration of suspended sediment in the reach	mg l^{-1}	Equation 24
V_r	Volume of water in the reach	mm	Equation 14

Table 5: Parameters and variables used in the in-stream sediment equations

The rate of change in SS mass with time is controlled by the difference between sediment input and output fluxes (Equation 19). Inputs from the terrestrial compartment, in-stream channel erosion and entrainment are grouped into a single input term, M_{input}, assumed to be related to in-stream flow using a power law (Equation 20). It was originally envisaged that Equation 19 would include separate terms for sediment delivery from the land (proportional to quick flow) and instream entrainment and erosion (proportional to instream discharge). However, adding a quick flow-dependent term to Equation 20 made little difference to model output and was therefore discarded, and the entrainment term was re-formulated to represent both terrestrial and instream inputs.

Equation 19: Rate of change in suspended sediment mass in the stream reach, M_{sus}, with time (kg day^{-1}), where superscript *i* denotes the land use class. f^i is one of f_{Ar}, f_{IG} or f_S.

$$\frac{dM_{sus}}{dt} = \left(\sum_i f^i M^i_{input}\right) + M_{sus,US} - M_{sus,DS}$$

Equation 20: Flux of sediment to the stream from terrestrial and in-stream sources, M_{input} (kg day^{-1})

$$M_{input} = E_{sus} Q_r^{k_M}$$

This simple treatment of the sediment inputs to the reach assumes that the majority of in-stream SS is generated from within- or near-channel sources, as is often observed (Bowes et al., 2005). A further assumption is made that these near-channel sediment sources are directly controlled by catchment erodibility and delivery to the watercourse, so that a change in terrestrial erodibility causes an instant reduction in in-stream SS concentration. This assumption is based on the observation that the coefficient in Equation 20, E_{sus}, relates to the erodibility of soils in the catchment (reviewed in Asselman, 2000). To build in a link between terrestrial processes and in-stream SS, the value of E_{sus} therefore incorporates data on the relative differences in expected erosion fluxes from different land units used in the Universal Soil Loss Equation (USLE; Kinnell, 2010; Renard et al., 1991; Wischmeier and Smith, 1965, 1978). E_{sus} is therefore calculated per land class (e.g. arable, improved grassland and semi-natural) and sub-catchment by multiplying a user-calibrated scaling factor with factors representing erodibility and sediment delivery to the stream (Equation 21). These factors include average slope (S_{SC}, which affects the transport capacity of quick flow), a

vegetation cover factor (C_{cover}) and a management factor ($C_{measures}$), all of which may vary with land use, and the cover factor may vary through the year if desired (Section 4.2.2).

Equation 21: Sediment-discharge rating coefficient, E_{sus}, (kg mm^{-1}), where superscript *i* indicates that the variable or parameter varies by land use, and superscript *j* by sub-catchment.

$$E_{sus}^{i,j} = E_M S_{reach}^{j} S_{SC}^{i,j} C_{cover}^{i} C_{measures}^{i}$$

The cover factor, C_{cover}, describes the ratio between the erodibility of a bare soil plot and the land use class; its value therefore ranges from 1 (maximum erodibility) to 0 (no erosion). Cover factors can be sourced from USLE-related literature reviews, selecting an appropriate geo-climatic region and range of vegetation and crop types. For example, Panagos et al. (2015) have collated crop type factors for typical European crops (Appendix, Table A1) and other European land cover (Appendix, Table A2). The user can also incorporate relative differences in inherent soil erodibility of different land classes into the relative differences in C_{cover}, i.e. differences due to soil properties such as texture and organic matter content (generally termed the *K* factor in USLE-related literature). A potential future extension to the model for areas which are dominated by semi-natural land could be to build in a link between the cover factor on semi-natural land and pressures which are known to increase soil erodibility such as grazing, burning and tree felling.

The management factor, $C_{measures}$, allows the user to explore the effects of sediment reduction measures and should be in the range 0 to 1, where 0 implies 100% reduction in sediment yield. Measures that could be taken into account could, for example, relate to the effects of tillage, cover crops or measures to reduce sediment connectivity to the stream (e.g. buffers or fences). The model requires the user to know the effectiveness of the chosen measure for a given land class. Values for effectiveness can be obtained for example from the USLE literature (e.g. Panagos et al., 2015) or from experimental work within the study catchment.

Sediment input to the watercourse should not only vary with terrestrial erodibility and transport capacity, but also with changes in in-stream inputs. A large body of empirical and theoretical work has shown that in-stream sediment transport is controlled by stream power, i.e. the rate of energy expenditure on the stream bed and banks (Bagnold, 1966). In-stream sediment inputs to the watercourse were therefore assumed to be proportional to stream power per unit length, $\omega=\rho g S_{reach} Q_r$. This equation includes terms for the density of water (ρ) and gravitational acceleration (g), both of which are constant and therefore grouped into the user-supplied scaling factor (E_M) in Equation 21. The remaining term, the reach slope (S_{reach}) is then an additional factor in Equation 21.

Additional sediment inputs to the stream reach are via flow from any upstream reaches and sediment is lost via flow from the reach (Equation 22). The integral of the flux out of the reach over each day, starting with an initial condition of 0, then provides a time series of the total sediment flux from the reach per day (Equation 23), which is used to calculate daily mean SS concentration (Equation 24). The latter is output by the model for comparison with observations.

Equation 22: Reach suspended sediment outflow from the reach bottom, $M_{sus,DS}$ (kg day^{-1})

$$M_{sus,DS} = \frac{M_{sus}}{V_r} Q_r$$

Equation 23: Rate of change in the flux of sediment from the reach, $M_{sus,tot}$ (kg day^{-1})

$$\frac{dM_{sus,tot}}{dt} = M_{sus,DS}$$

Equation 24: Mean daily concentration of SS in the stream reach, SS_r (mg l^{-1})

$$SS_r = \frac{M_{sus,tot}}{Q_{r,av}} \frac{1}{A_{SC}}$$

Connectivity between sediment source areas and the water course is an important factor in determining sediment yield to a water course. This is not explicitly accounted for at present, although it is indirectly included in the value assigned to the scaling factor, E_M, in a given area. A potential improvement would be to explicitly include a connectivity factor in Equation 20, for example by: (1) using drainage density as a proxy for connectivity, (2) only considering the characteristics of land within a certain distance of a drainage ditch/watercourse, as land most likely to be a potential sediment source area; (3) factoring in field size and the presence of barriers to flow such as walls and hedges; (4) calibrating the sediment yield scaling factor by sub-catchment, rather than keeping it constant over the whole catchment. In addition, the sub-catchment slope factor could be altered to be more representative of potential sediment source areas, for example it could be the average slope of land within a certain distance of a watercourse.

Assuming that the amount of sediment in near-channel sources is directly proportional to terrestrial erodibility is a big simplification. An implication of this assumption is that a reduction in terrestrial erodibility causes an instant reduction in in-stream SS concentration. In reality, hysteresis is often seen in the sediment-discharge relationship, reflecting the change in sediment source distance or supply during a rainfall event (e.g. Oeurng et al., 2010). As the store of sediment in near-channel sources is not tracked, there is no ability to simulate source-exhaustion over successive storm events (Bowes et al., 2005). Test applications are required to determine whether this is an issue in a given study catchment. Over the longer term, we might expect a time lag between changes in erodibility and in-stream effects as in-stream sources become exhausted. For example, typical lag times of decades or more have been reported for the retention of bulk sediment in river channels (Trimble, 2010). However, here we are primarily concerned with the fine sediment fraction (silt and clay), as the fraction that is of greatest significance for P transport due to its relatively high P content. This finer sediment fraction is substantially more mobile, with residence times of less than a year reported for many rivers, excluding storage on floodplains (Sharpley et al., 2013, and references therein).

Other issues with this simple formulation are that sediment deposition is not explicitly accounted for, and so the model cannot simulate a net flux of sediment from the water column to the stream bed. This could be a problem in some areas, for example in catchments with a big difference in slope and sediment supply between reaches. Future work is needed to determine under which circumstances deposition needs taking into account, and how it should best be done in the simplest way possible. Another potential future improvement could be to split bank erosion and entrainment from terrestrial delivery. Bank erosion and entrainment may be a key sediment input (Lefrançois et al., 2007), and assuming terrestrial sediment reduction measures cause a proportional reduction in in-stream sediment load ignores the fact that bank erosion will be unaffected by these measures. Finally, the instream sediment equations only consider allochthonous particles sourced from the catchment. However, autochthonous particles, generated in-stream by biological processes, may make up an important part of suspended matter (Stutter et al., 2009), and in some areas it may be appropriate to consider both.

4.2.2 Dynamic cover factor

On arable land, the key risk period for soil erosion is between preparation of the seed bed and establishment of the crop, when fine ploughing results in bare soils with low cohesion. To take this temporal change in erodibility into account in the model, there is the option to replace the user-supplied constant cover factor on arable land (hereafter termed $C_{cov,av}$) with a dynamic factor, which changes during the course of the year (hereafter termed C_{cover}). This dynamic cover factor is calculated so that its annual average is the user-specified cover factor, to preserve the user's knowledge of the ratio in long-term erodibility between land use classes. In most temperate areas, high-risk seed beds will be present during both spring and autumn, as many farmers cultivate a mixture of spring- and autumn-sown crops. Arable land may therefore be further sub-

divided into spring-sown (e.g. spring cereals) and autumn sown (e.g. winter cereals) if the user wishes to take dynamic erodibility into account.

Two options were explored for calculating the dynamic cover factor (associated parameters and variables are defined in Table 6). The first approach uses a cosine wave (Equation 25). This is appealing in that it is smooth and only requires one user-supplied parameter, the date of maximum erodibility. In much of northern Europe, for example, this could be around the end of February (day 60) for spring-sown crops and the end of October (day 300) for autumn-sown crops. The amplitude of the curve can be fixed to ensure that the annual mean is equal to $C_{cov,av}$ (Equation 25). The downside of this formulation is that it assumes that points of maximum and minimum erodibility are half a year apart. For autumn-sown cereals in particular this is unlikely.

Variable	Description	Units	Source
C_{cover}	Erosion soil cover factor	None	Equation 26 (if dynamic) or $C_{cover,av}$
$C_{cover,av}$	Average soil cover factor for erodibility	None	Input parameter
$C_{measures}$	Erosion management factor	None	Input parameter
$d_{E,max}$	Date of maximum soil erodibility	None	Input parameter (for spring- and autumn-sown)
$d_{E,start}$	Start of the high erodibility period	None	Model calculates ($D_{E,max}$ -30)
$d_{E,end}$	End of the high erodibility period	None	Model calculates ($D_{E,max}$+30)
d_{year}	Julian day of the year	None	Model calculates
f_{spr}	Fraction of arable land that is spring sown	None	Input parameter

Table 6: Parameters and variables used in the erodibility equations

Equation 25: Dynamic crop cover factor for arable land calculated using a cosine wave, where superscript *i* indicates the crop type (spring-sown or winter-sown)

$$C_{cover}^{i} = \frac{C_{cov,av}^{i}}{2}\left(\cos\left(\frac{2\pi}{365}d_{year} + d_{Emax}^{i}\right) + 1\right)$$

The alternative approach adopted instead was to assume a constant cover factor throughout the year, apart from during a high risk period defined by a user-specified maximum erodibility date. Within this high risk period, the factor follows a triangular shape (Figure 8), which smooths the transition from lower to higher erodibility risk, to take into account differences in ploughing dates across the catchment. The difference between $C_{cov,av}$ and the dynamic cover factor outside the high risk period is calculated so that the annual average of the dynamic cover factor equals $C_{cov,av}$ (Figure 8 and Equation 26). To provide comparable simplicity to the sine curve option, the length of the high erodibility period is fixed. This period should encompass the likely variability in seed bed presence in both space and time in the catchment, whilst not being so wide as to reduce the cover factor during the remainder of the year to below the average values on improved grassland and semi-natural land – we would generally expect arable land, with its higher proportion of bare soil, compaction and tramlines, to have higher erosion risk than the other two land classes. A period of two months (60 days) provided a good compromise, although the sensitivity of the model to this factor could be assessed in the future. Within the high risk period, the value of the dynamic cover factor is then calculated by linear interpolation (Equation 26), and the results for spring- and autumn-sown crops are averaged to give the overall factor to be used in Equation 21.

Equation 26: Dynamic cover factor for arable land, C_{cover}, calculated using a triangular wave during the high risk period, where superscript *i* indicates the crop type (spring-sown or winter-sown)

If the day of the year, d_{year}, is within the period $d_{E,max}{}^{i}$ ± 30 days:

$$\text{If } d_{year} < d_{E,max}\text{: } C_{cover}^{\,i} = C_{cov,av}^{i} + \frac{\left(1 - C_{cov,av}^{i}\right)\left(d_{year} - d_{E,start}^{i}\right)}{d_{E,max}^{i} - d_{E,start}^{i}}$$

$$\text{If } d_{year} > d_{E,max}\text{: } C_{cover}^{\,i} = 1 + \frac{\left(C_{cov,av}^{i} - 1\right)\left(d_{year} - d_{E,max}^{i}\right)}{d_{E,end}^{i} - d_{E,max}^{i}}$$

Otherwise:

$$C_{cover}^{i} = C_{cov,av}^{i} - \left(\frac{60\left(1 - C_{cov,av}^{i}\right)}{2(365 - 60)}\right)$$

Averaging over arable land classes:

$$C_{cover} = f_{spr} C_{cover}^{spring} + \left(1 - f_{spr}\right) C_{cover}^{autumn}$$

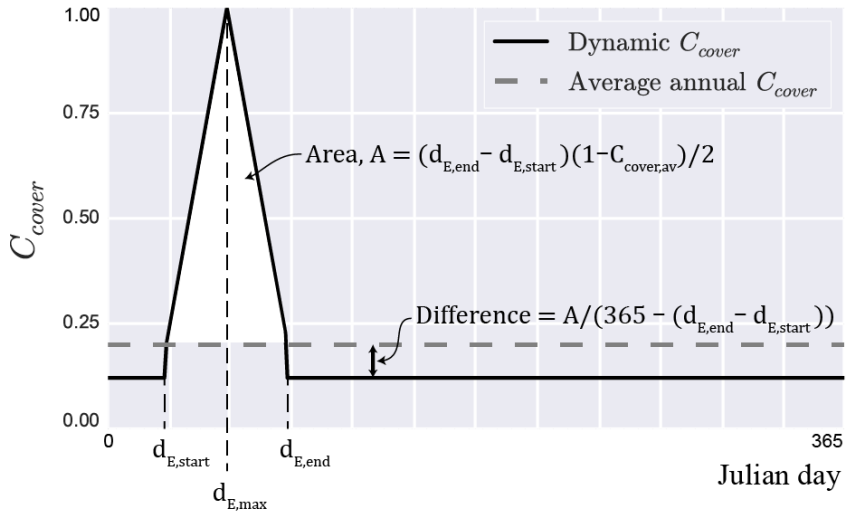

Figure 8: Schematic illustrating the shape of the dynamic crop cover factor (C_{cover}) over a year. The period of high erodibility starts on $d_{E,start}$, is at its maximum at $d_{E,max}$ and finishes at $d_{E,end}$.

Model testing, preferably in a formal statistical framework, is required to determine whether the additional complexity of the dynamic cover factor is warranted. A good place to test this would be in an area where sediment fluxes are believed to change throughout the year in response to changing arable crop cover. It would also be worth exploring how suitable the dynamic cover factor formulation is for autumn-sown crops, which are likely to have relatively bare soils throughout the winter.

4.3 Phosphorus processes

4.3.1 Soil processes

a) Overview

Soil P processes are calculated separately for two land use classes – a 'high P' class and a 'low P' class. Below, the high P class is referred to as agricultural land, and the low P class as semi-natural, but other land uses could be assigned to these classes. For particulate P fluxes, a further distinction may be made between high and low erodibility land uses in the high P class, e.g. between arable and improved grassland, to take the different erodibility (and therefore sediment and PP transport) into account (Section 4.2.1). The model also includes the ability to simulate semi-natural land newly-converted from agricultural land and vice versa (discussed further in Section 4.3.1 c).

In the model, P is present in the soil in three forms: (1) dissolved P (TDP) in the soil water, (2) labile soil P, which can take part in sorption reactions with soil water TDP, and (3) inactive soil P. The masses of dissolved and labile soil P change through time, whilst the mass of inactive soil P is constant. Parameters and variables used in the soil P equations are defined in Table 7.

Variable	Description	Units	Source
A_{SC}	Sub-catchment area	km^2	Input parameter
β	Baseflow index	None	Input parameter
dP_{labile}/dt	Rate of change of labile soil P mass with time	kg day^{-1}	Equation 33
$dTDP_s/dt$	Rate of change of soil water TDP mass with time	kg day^{-1}	Equation 34
EPC_0	Agricultural soil equilibrium P concentration of zero sorption	kg mm^{-1}	Equation 29 or $EPC_{0,user}$
$EPC_{0,user}$	User-supplied initial EPC_0 for agricultural soil	mg l^{-1}	Input parameter
f_i	Fraction of land use in each of the possible land use classes, *i*, including agricultural (A; $f_{Ar} + f_{IG}$), arable (Ar), improved grassland (IG), semi-natural (SN), and newly-converted versions of all 3 (NC_i)	None	Input parameters
K_f	Soil P adsorption coefficient	mm kg $soil^{-1}$	Equation 28
M_{soil}	Soil mass	kg	Equation 32
$M_{soil,m2}$	Soil mass per m^2 (soil depth × bulk density)	kg m^{-2}	Input parameter
$P_{inactive}$	Soil inactive P mass	kg	Equation 30
P_{labile}	Soil labile P mass	kg	Equation 33
$P_{labile,0}$	Initial soil labile P content	kg	Equation 31
$P_{netInput}$	Net annual input (or uptake) of P to the land class	kg ha^{-1} yr^{-1}	Input parameter
$P_{soilConc,A}$	Total soil P content in agricultural land as a mass ratio	mg P (kg soil)$^{-1}$	Input parameter
$P_{soilConc,S}$	Total soil P content in semi-natural land as a mass ratio	mg P (kg soil)$^{-1}$	Input parameter
Q_q	Quick flow	mm day^{-1}	Equation 5
Q_s	Soil water flow	mm day^{-1}	Equation 10
$TDP_{g,conc}$	Groundwater TDP concentration	mg l^{-1}	Input parameter
$TDP_{g,land}$	Groundwater TDP input to the reach	kg day^{-1}	Equation 37
$TDP_{q,land}$	Quick flow TDP input to the reach	kg day^{-1}	Equation 36
TDP_s	TDP mass in the soil water	kg	Equation 34
$TDP_{s,land}$	Soil water TDP input to the reach	kg day^{-1}	Equation 35
V_s	Soil water volume	mm	Equation 6

Table 7: Parameters and variables used in the soil and groundwater P equations

b) Interactions between soil P and dissolved soil water P

The labile soil P store and dissolved P in the soil water are assumed to be in equilibrium, and a simple linear relationship is used to relate soil total P concentration and EPC_0, the equilibrium TDP concentration at which there is no net sorption or desorption of P (Equation 27; Figure 9). This relationship can be conceptualised as accounting for sorption and mineralization/immobilization reactions. This linear relation cannot simulate P saturation, but because of its simplicity it is recommended for use in catchment models, as long as soil water TDP concentration is below 1 to 10 mg l^{-1} (McCray et al., 2005).

Equation 27: Relationship between soil P content ($P_{soil,conc}$; kg P kg $soil^{-1}$) and soil water TDP concentration (expressed as the equilibrium P concentration, EPC_0; kg mm^{-1})

$$P_{soil,conc} = K_f EPC_0 + 10^{-6} P_{soilConc,S}$$

Soil water in semi-natural areas tends to have low TDP concentrations (Q_{75}<5 μg l^{-1}; unpublished James Hutton Institute data), implying tight retention of any P released from the soil matrix. It is therefore assumed that semi-natural land does not contain labile soil P, that semi-natural soil water TDP concentration is zero, and that all soil P in semi-natural land is in the inactive soil P store (Equation 30). The soil P content of semi-natural land is therefore used as the y-axis intercept in Equation 27, and the inactive soil P store on agricultural land is assumed to be the same as in semi-natural land (Figure 9).

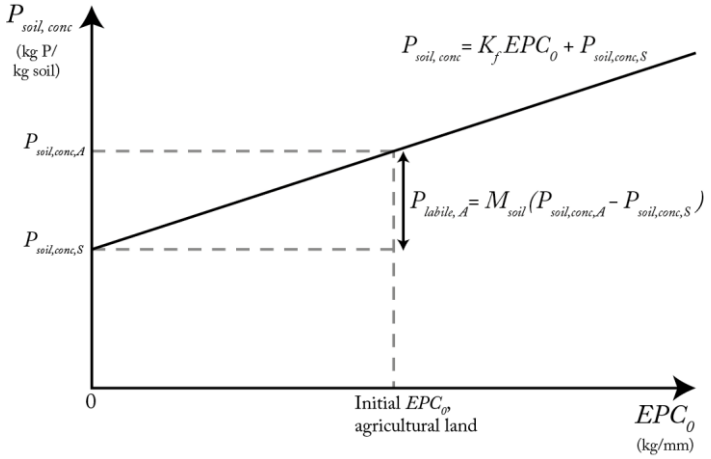

Figure 9: Illustration of the conceptual model used to link soil P content and soil water TDP concentration, expressed as EPC_0, the equilibrium TDP concentration of zero sorption.

Having defined the y-intercept, there are then two unknowns in Equation 27 for a given soil total P content: the adsorption coefficient (K_f) and EPC_0. It is very important for simulated soil water TDP concentrations to be in the right range, as in diffuse pollution-dominated systems near-surface soil water flow often controls in-stream TDP peaks. Initial agricultural soil water TDP concentration, assumed to be equivalent to soil water EPC_0, was therefore chosen to be the calibrated parameter, and K_f is calculated internally by the model using Equation 28. Once agricultural EPC_0 has been determined through calibration, K_f output by the model from the calibration period is then supplied as an input parameter for model runs in simulation mode and EPC_0 is calculated instead within the model (Equation 29). Initial EPC_0 is still an input parameter in any validation and scenario runs, but merely to provide the initial conditions for the soil water P content. This formulation removes much of the need for careful thinking and parameterisation from the modeller, thereby reducing the risk of highly inappropriate sorption equations, and therefore unrealistic simulations of the impacts of changes in fertilizer or manure inputs or land use change.

Equation 28: The adsorption coefficient, K_f (mm kg soil^{-1}), calculated during the calibration period

$$K_f = \frac{10^{-6}\left(P_{soilConc,A} - P_{soilConc,S}\right)}{EPC_0}$$

Equation 29: EPC_0, the equilibrium TDP concentration of zero sorption (kg mm^{-1} in the equation below; supplied by the user in mg l^{-1}). N.B. the user may also opt for EPC_0 to be constant

$$EPC_0 = \frac{P_{labile}}{K_f M_{soil}}$$

Having assumed that the inactive soil P store on agricultural land is equivalent to the total soil P content on semi-natural land, initial labile P content in agricultural land is then calculated as the difference between cultivated and semi-natural total P content (Equation 31). This assumption is only appropriate if soils under the two land classes have similar P sorption capacity (controlled primarily by iron oxide and clay content).

Equation 30: Inactive soil P content in agricultural and semi-natural land, $P_{inactive}$ (kg)

$$P_{inactive} = 10^{-6} P_{soilConc,S}\, M_{soil}$$

Equation 31: Initial labile soil P content in agricultural land, $P_{labile,0}$ (kg)

$$P_{labile,0} = 10^{-6}\left(P_{soilConc,A} - P_{soilConc,S}\right) M_{soil}$$

Converting from soil P concentration to mass of P in the labile and inactive stores requires an estimate of the sub-catchment soil mass (Equation 32). The user-specified areal soil mass parameter ($M_{soil,m2}$) can be

calculated by multiplying soil bulk density with an estimate of soil depth; topsoil depth is recommended, being the depth of soil which contains highest soil P concentrations. These two parameters are lumped together as one user input parameter to reduce parameter non-identifiability issues during auto-calibration.

Equation 32: Sub-catchment topsoil mass, M_{soil} (kg)

$$M_{soil} = M_{soil,m^2} 10^6 A_{SC}$$

The change in mass of P in the labile P store due to a change in TDP concentration in the soil water can then be calculated and is assumed to control the rate of change in soil labile P in agricultural land with time (Equation 33). Inputs from fertilizer and manure are all assumed to occur in liquid form and to bring about an increase in labile P mass through adsorption. Conversely, a change in labile P content may cause a change in soil water TDP concentration due to a shift in EPC_0 (Equation 29). The model also includes the option for EPC_0 to be constant over time, to simplify the model for short model runs where no shift in soil water TDP concentration is expected.

Equation 33: Rate of change in soil labile P mass, P_{labile}, with time (kg day^{-1})

$$\frac{dP_{labile}}{dt} = K_f M_{soil} \left(\frac{\mathrm{TDP}_s}{V_s} - \mathrm{EPC}_0 \right)$$

The rate of change of soil water TDP mass with time in agricultural land is controlled by the balance of input and output fluxes (Equation 34). Potential inputs are from the application of fertilizer and manure and net release of soil P. Outputs are via plant uptake, sequestration into soil P, soil water flow and quick flow. The latter is included as it is assumed that quick flow also inherits soil water TDP concentration. Fertilizer, manure and plant uptake fluxes are grouped together into a single annual P budget parameter ($P_{netInput}$; kg ha^{-1} yr^{-1}), which is then evenly applied (or subtracted, if there is net output) over the course of the year. This grouping greatly reduces the number of parameters required, and the $P_{netInput}$ parameter may be readily informed by budgeting studies or published national P surplus values (e.g. eurostat, 2013). This simplified treatment of terrestrial P inputs and outputs assumes a relatively constant TDP concentration in soil water throughout the year. Whilst this is clearly a simplification, previous modelling work has suggested the additional complexity involved in attempting to simulate the daily changes in soil water TDP concentration in response to variations in fertilizer, manure and plant uptake fluxes is not justified (Jackson-Blake et al., 2015). At present the model takes as input a single constant value. An easy future extension to the model would be to provide the option for this to be replaced by an annual time series of values.

Equation 34: Rate of change of soil water TDP mass, TDP_s, with time (kg day^{-1})

$$\frac{d\ \mathrm{TDP}_s}{dt} = \frac{100\ A_{SC}}{365} P_{netInput} - \frac{dP_{labile}}{dt} - Q_s \frac{\mathrm{TDP}_s}{V_s} - Q_q \frac{\mathrm{TDP}_s}{V_s}$$

This representation of soil P processes greatly simplifies the actual processes involved. In reality soil P is present in a continuum of interlinked states of varying extractability, and hysteresis effects are common in P transfers between the states. However, the understanding of how detailed soil chemical processes upscale to the catchment-scale is arguably not yet advanced enough for fine-scaled geochemical principles to be usefully incorporated into a catchment-scale model, and there is certainly a lack of data to constrain such processes at a catchment scale. A potential future change to the model would however be to use more detailed geochemical models or lab experiments to derive isotherm parameters for a suite of soil types, using soil properties such as Fe and Al oxide content (Dari et al., 2015).

Example soil P results for agricultural soils in the Tarland catchment are shown in Figure 10, assuming an initial labile soil P content of 585 mg kg^{-1}, an initial EPC_0 of 0.1 mg l^{-1}, soil depth of 9.5 cm and annual net P inputs of 10 kg ha^{-1} yr^{-1}. Soil water TDP concentrations are slightly higher than the EPC_0 because of P inputs to the soil water, resulting in net adsorption and a gradual increase in labile P and EPC_0 over time.

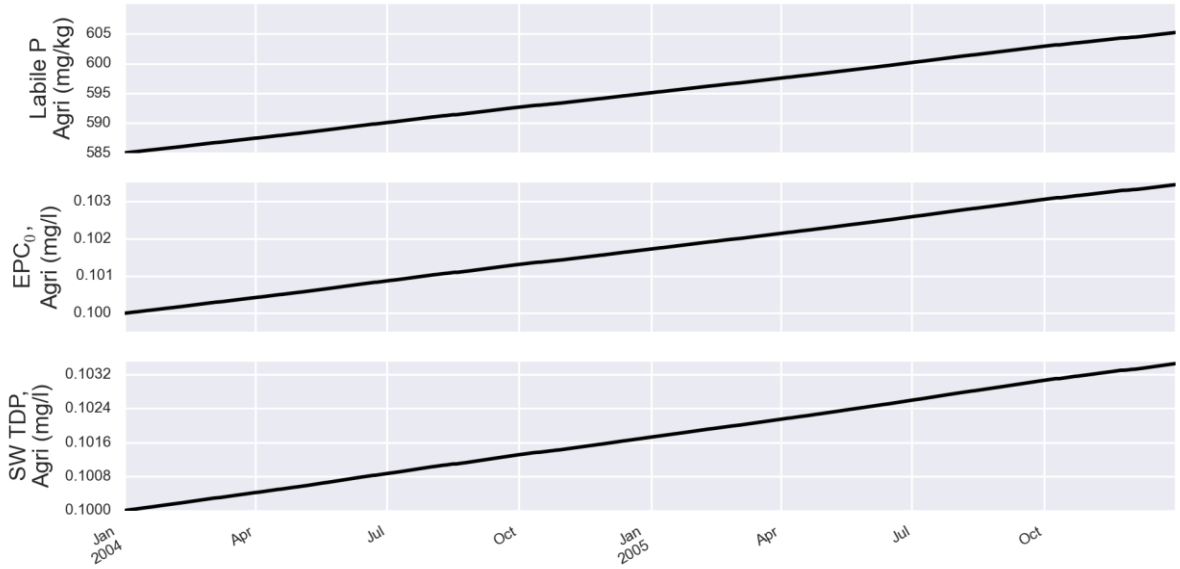

Figure 10: Simulated change in agricultural soil labile P content, soil water (SW) EPC_0 and soil water TDP concentration over a two year period, assuming a soil depth of 9.5 cm and net P inputs of 10 kg ha^{-1} $year^{-1}$.

c) Newly-converted land

A potential use of the model is to explore the impact of land use change on surface water P concentrations and loads. This land use change could be the conversion of agricultural land to semi-natural land, or vice versa. Land that has recently changed use will retain many of its previous characteristics, and cannot therefore be grouped with long-established land of the same use. Of particular importance for P and water quality is legacy soil P, the store of P that builds up in agricultural soil over years of high P application rates. Such legacy P may result in sustained high leaching and PP losses from old agricultural land potentially for several decades after reductions in fertilization (Jarvie et al., 2013b). Likewise the lack of legacy soil P in new agricultural land, recently converted from semi-natural land, may result in low P losses compared to well-established agricultural land.

To allow such effects to be simulated, a third 'newly-converted' land class was introduced into the model. Within each sub-catchment, this newly-converted land can be either semi-natural (initial labile soil P is equivalent to that on agricultural land) or agricultural (no labile soil P at the start of the model run). Two additional ODEs are then introduced: the change in labile soil P on newly-converted land with time and the change in soil water TDP with time. These take the same form as Equation 33 and Equation 34, respectively. EPC_0 is also calculated for the newly-converted class, and there is one additional user-input parameter, $P_{netInput}$. On new semi-natural land this is likely to be a negative, with net uptake of P from the soil. Otherwise, newly converted semi-natural land is grouped with existing semi-natural land, and likewise for agricultural, for other parameterisations and processes.

d) TDP flux to the stream from soil water and quick flow

The TDP input to the stream transported by soil water flow is calculated by summing the inputs from agricultural land and any newly-converted semi-natural or agricultural land (Equation 35).

Equation 35: TDP input to the reach from soil water flow, $TDP_{s,land}$ (kg day^{-1}), where *i* denotes the land use class (*A*: agricultural, *NC*: newly-converted semi-natural or agricultural)

$$\mathrm{TDP}_{s,land} = \sum_{i=A,NC} f_i(1-\beta)Q_s\left(\frac{\mathrm{TDP}_s^i}{V_s}\right)$$

The flux of TDP to the water course from the reach via quick flow is given by Equation 36. The majority of the flow pathways that make up quick flow inputs to the stream interact with the soil surface (e.g. infiltration and saturation excess flow) or are sourced from soil water (e.g. tile drainage). It was therefore assumed that quick flow inherits soil water TDP concentration. This may be conservative in areas where there is substantial runoff from farmyards, which may have TDP (and PP) concentrations which are well above those found in soil water, or if quick flow events occur directly after fertilizer or manure are applied.

Equation 36: Quick flow TDP input to the reach from the land, $TDP_{q,land}$ (kg day^{-1}), where *i* denotes the land use class (*A*: agricultural, *NC*: newly-converted semi-natural or agricultural)

$$\mathrm{TDP}_{q,land} = \sum_{i=A,NC} f_i \, Q_q \left(\frac{\mathrm{TDP}_s^i}{V_s} \right)$$

e) Incorporating soil test P data

Soil P content is usually measured for agronomic purposes, where the aim is to measure plant-available P to help choose appropriate fertilizer application rates. Many procedures exist which aim to determine plant-available soil P; indeed, there are more than ten official methods used in Europe alone (Jordan-Meille et al., 2012). This soil test P data is much more common than total soil P data, so it would be useful for the model to be able to incorporate soil test P data, rather than relying on total soil P data alone. In principle soil test P could replace labile soil P in Equation 27, as long as two additional relationships can be defined:

(1) A relationship between soil test P and total soil P, as total soil P content is still required for the PP simulation. There is always likely to be considerable scatter in this relationship due to varying soil chemistry, composition and texture. An analysis of Scottish soils data, for example, revealed a weak but significant relationship between total soil P and Modified Morgan's P: $P_{total} = 61.1\, P_{soilTest} + 529$ (n=77, R^2=0.62, p<0.001), although as is clear in Figure 11, the uncertainty in total P predictions based on this equation would be substantial.

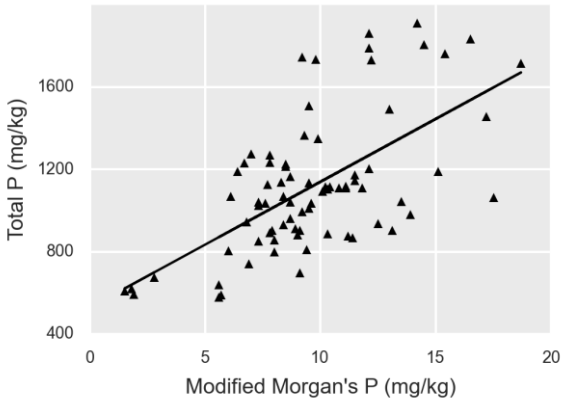

Figure 11: Relationship between soil test P (Modified Morgan's P) and total soil P from a range of Scottish soils (M. Stutter, pers. comm.)

(2) A relationship describing the proportion of net total P inputs (e.g. from fertilizer and manure minus uptake) that enters the labile, soil test P store. Model testing showed that this ratio cannot be the same as that derived from the relationship between soil test P and total soil P. If this ratio were the same, a total P to soil test P ratio of around 60 (from the Scottish soils dataset above) would imply that 1/60th of net total P inputs enter the available P store. However, with a net P input of 10 kg ha^{-1} yr^{-1} (typical for Scottish catchments), model testing showed that a ratio of <25 is required to maintain plant-available P stores at their present-day value, and that the model is extremely sensitive to the value chosen.

The fact that these two additional relationships must be independently specified causes an increase in model complexity that was not felt to be justified by an increase in model realism. In particular, if linear relationships are used to relate total soil P and soil test P, and to relate soil test P and soil water EPC_0, then by definition there will also be a linear relationship between total soil P and soil water EPC_0, meaning the increase in complexity is not justified. It was therefore decided to maintain the model structure described in Section 4.3.1 (b). However, if soil test P data are available instead of total soil P data for a given area, the user could use a linear regression between soil test P and total soil P to derive the latter (e.g. using the regression derived above for Scottish soils data). A potential future extension to the model is for this calculation to be performed internally, using user-specified regression coefficients.

4.3.2 Groundwater phosphorus

The concentration of TDP in groundwater, as in soils, depends on historic P inputs and the P sorption capacity of the aquifer matrix. The latter is often largely controlled by the iron oxide content of the aquifer, with groundwater pH and dissolved oxygen content also playing an important role (Domagalski and Johnson, 2011), whilst co-precipitation with calcium carbonate is important in calcareous aquifers. These processes substantially reduce P mobility within the sub-surface, and traditionally groundwater has therefore only been considered to have negligible TDP concentrations and to dilute surface water P concentrations. However, it is now being increasingly recognised that groundwater TDP concentrations can become elevated by anthropogenic activities (e.g. Holman et al., 2008). Some areas in which groundwater has become enriched in P, for example due to elevated agricultural P inputs or prolonged disposal of sewage effluent, may potentially become net sources of P for decades after the original source of P has been removed (Stollenwerk, 1996).

Ideally, the model would therefore include a link between soil water and groundwater TDP concentrations, taking into account aquifer and groundwater geochemistry. However, the process-understanding needed to formalise this link is arguably not yet developed enough, and certainly the data on groundwater and aquifer geochemistry is hard to come by in many areas. There are therefore good practical reasons for adopting a simpler approach which does not take this process understanding into account. In addition, changes in groundwater TDP concentration over time are likely to be slow, being buffered by potentially large groundwater residence times and sorption reactions, and smaller than associated changes in soil water and effluent fluxes which will drive any changes in groundwater state. For these reasons, a very simplistic approach is taken in the model: dissolved P transport to the stream occurs via groundwater flow, but groundwater TDP concentration is assumed to be constant through time, maintained at a user-specified value ($TDP_{g,conc}$; Equation 37. Variables are defined in Table 7).

Equation 37: Groundwater TDP input to the reach, $TDP_{g,land}$ (kg day^{-1})

$$\mathrm{TDP}_{g,land} = A_{SC} Q_g \mathrm{TDP}_{g,conc}$$

This simplistic approach is a good starting point, but is only valid where the groundwater TDP concentration is indeed unlikely to change over the course of the model run. This is likely to be the case over sub-decadal time periods, in areas with large aquifers, where the groundwater matrix is rich in Fe oxides and/or where the groundwater is oxic. Caution should otherwise be employed. This is a potential area for future model development, the ultimate aim being to derive a simple relationship between soil water and groundwater TDP concentration using readily-measurable groundwater properties. A linear relationship could be a suitable starting point. The gradient of the line could be derived by making some assumptions to help estimate the location of two points on the line: point 1 could be current measured groundwater TDP concentration, corresponding with sub-catchment averaged soil water TDP concentration. The second point would require an estimate of the 'pristine', non-anthropogenic groundwater TDP concentration (e.g. based on space-for-time substitution of measured data), associated with soil water TDP concentrations in semi-natural land, plus knowledge or assumptions of the time taken for semi-natural groundwater to reach its current state.

4.3.3 In-stream phosphorus

The in-stream P process model simulates in-stream dilution of diffuse and point source P inputs and down-stream transport. Parameters and variables used in the in-stream P equations are defined in Table 8.

Variable	Description	Units	Source
A_{SC}	Sub-catchment area	km^2	Input parameter
dPP_r/dt	Change of PP mass in the reach with time	kg day^{-1}	Equation 40
$dPP_{r,df}/dt$	Daily flux of PP from the stream reach	kg day^{-1}	Equation 41
$dTDP_r/dt$	Rate of change of TDP mass in the reach with time	kg day^{-1}	Equation 38
$dTDP_{r,df}/dt$	Daily flux of TDP from the stream reach	kg day^{-1}	Equation 41
E_{PP}	Particulate P enrichment factor	None	Input parameter
f_i	Fraction of land use in each of the possible land use classes, *i*, including agricultural (A; $f_{Ar} + f_{IG}$), arable (Ar), improved grassland (IG), semi-natural (SN), and newly-converted versions of all 3 (NC_i)	None	Input parameters
M_{input}	Sediment mass input to the reach from the land and in-stream entrainment	kg day^{-1}	Equation 20
M_{soil}	Soil mass	kg	Equation 32
$P_{inactive}$	Soil inactive P mass	kg	Equation 30
P_{labile}	Soil labile P mass	kg	Equation 33
PP_{input}	PP input to the reach from the land and in-stream entrainment	kg day^{-1}	Equation 39
PP_r	Mass of PP in the reach	kg	Equation 40
$PP_{r,conc}$	Daily mean concentration of PP in the reach	mg l^{-1}	Equation 42
$PP_{r,df}$	Mean daily flux of PP from the reach	kg day^{-1}	Equation 41
$PP_{r,US}$	PP input to the reach from upstream reaches	kg day^{-1}	Model calculates
Q_q	Quick flow	mm day^{-1}	Equation 5
Q_r	Instantaneous reach discharge	mm day^{-1}	Equation 17
$Q_{r,av}$	Daily mean reach flow	mm day^{-1}	Equation 18
TDP_{eff}	Effluent TDP input to the reach	kg day^{-1}	Input parameter
$TDP_{g,land}$	Groundwater TDP input to the reach	kg day^{-1}	Equation 37
$TDP_{q,land}$	Quick flow TDP input to the reach	kg day^{-1}	Equation 36
TDP_r	Mass of TDP in the reach	kg	Equation 38
$TDP_{r,conc}$	Daily mean concentration of TDP in the reach	mg l^{-1}	Equation 42
$TDP_{r,df}$	Mean daily flux of TDP from the reach	kg day^{-1}	Equation 41
$TDP_{r,US}$	TDP input to the reach from upstream reaches	kg day^{-1}	Model calculates
$TDP_{s,land}$	Soil water TDP input to the reach	kg day^{-1}	Equation 35
V_r	Reach volume	mm	Equation 14

Table 8: Parameters and variables used in the in-stream P equations.

a) TDP

The rate of change in instream TDP mass with time depends on the difference between input and output fluxes. A simplistic representation is used, where inputs are from the land phase (quick, soil water and groundwater flow), sewage and upstream reaches, and the only output is reach outflow (Equation 38).

Equation 38: Rate of change in reach TDP mass, TDP_r, with time (kg day^{-1})

$$\frac{d\,\mathrm{TDP}_r}{dt} = \mathrm{TDP}_{q,land} + \mathrm{TDP}_{s,land} + \mathrm{TDP}_{g,land} + \mathrm{TDP}_{eff} + \mathrm{TDP}_{r,US} - Q_r \frac{\mathrm{TDP}_r}{V_r}$$

This simple formulation assumes that instream TDP is in a state of dynamic equilibrium, i.e. instream sinks of TDP (e.g. adsorption and biological uptake) are balanced by instream sources (e.g. desorption and mineralisation). Studies have indicated that this balance between sources and sinks may in fact change through the year in response to changing concentrations (e.g. Stutter and Lumsdon, 2008). Retention is thought to be particularly important during low flows, due to biological uptake and sorption (House, 2003). Omitting TDP sinks from the model could therefore result in other P sources being over-estimated, particularly groundwater and effluent inputs. To determine whether an in-stream TDP sink is significant in a particular study catchment, data are needed to quantify the sink directly or to provide good constraints on groundwater and effluent inputs. In-stream processes may also become net sources or sinks of TDP if

equilibrium has not yet been reached or is disturbed, e.g. by a change in external loading. For example, reducing effluent P inputs may cause a reduction in water column TDP concentration, which may cause P-enriched bed sediments to release TDP until a new equilibrium state is reached (Stutter et al., 2010). By not incorporating this potential interaction between bed sediments and the water column, the model is not able to represent legacy sewage effluent P. However, as explained in Section 3.1, this legacy store is thought to be much smaller than other potential legacy P stores in the catchment, and to have a more rapid turnover time.

In many countries, soluble reactive P (SRP) is used by regulators to assess compliance with water quality standards, rather than TP or TDP. It is therefore desirable to be able to convert TDP to SRP. Models such as INCA-P do this using a simple linear regression with regression parameters supplied by the user. This approach works well in the majority or rivers, and as a starting point is recommended here. It has not been coded into the model, but the user can easily transform model output using their own regression equation. Different TDP sources may have very different SRP:TDP ratios, and a potential future extension could be to factor in different SRP:TDP ratios of different P sources.

b) PP

All PP is assumed to be sediment-bound, and so PP inputs to the water column are assumed to be proportional to sediment inputs (Equation 39). The mass of PP input to the stream is therefore simply the mass of sediment transported to the stream from each land use class, M_{input}, multiplied by the P content of the soil in that class and assuming unlimited soil P. This approach has the same limitations and caveats as the sediment equations (Section 4.2.1). It also assumes that changes in the P content of soils are instantly reflected in the composition of in-stream sediments, discounting time lags or potential in-stream PP stores. In-stream stores of P are relatively small and short-lived compared to terrestrial stores (Jarvie et al., 2013a), so it was felt that the additional complexity needed to account for these in-stream processes was not justified.

Equation 39: PP input to the reach, PP_{input} (kg day^{-1}), where superscript i denotes the land use class

$$\mathrm{PP}_{input} = E_{PP}\, M^{i}_{input} \sum_{i} f^{i} \frac{\left(P^{i}_{labile} + P_{inactive}\right)}{M_{soil}}$$

An enrichment factor, E_{PP}, represents the selective delivery to the stream of finer particles enriched in P compared to source soils (Sharpley, 1980). The use of a constant enrichment factor is a simplification; in reality there is a well-documented decrease in PP loss with increasing erosion (Radcliffe and Cabrera, 2006). This is because as runoff and erosion increase there is less particle size sorting, so P-enriched finer sediment makes up a smaller proportion of the total sediment mobilised. When assembling enrichment ratio information for the CREAMS model, Menzel (1980) concluded that a log-relationship between enrichment ratio and sediment yield appears to hold in a variety of conditions: $\ln(E_{PP}) = 2.00 - 0.16\ln(Y_{sed})$, where Y_{sed} is the sediment yield (kg ha^{-1}). A potential future extension to the model would be to investigate whether this additional complexity is warranted in some areas.

In Equation 39, PP inputs to the stream are summed over up to six land use classes: arable, improved grassland, semi-natural, and newly-converted versions of each (Section c). The sediment flux for newly-converted land corresponds to the same flux for established land. The rate of change in the mass of PP in the water column with time is then given by Equation 40. As with TDP, a simplistic representation of the associated fluxes is adopted: inputs are from the land phase and entrainment (grouped as one flux) and upstream reaches; the only output is via outflow from the reach. Sewage PP inputs are not included, as the majority of effluent P tends to be in dissolved form (Neal et al., 2005; Withers and Jarvie, 2008). As a starting point, in-stream desorption of TDP from PP is not accounted for. This is likely to be justified in rivers with relatively short residence times, but potentially less so in larger, slower-flowing rivers.

Equation 40: Rate of change in reach PP mass, PP_r, with time (kg day^{-1})

$$\frac{d\,\mathrm{PP}_r}{dt} = \mathrm{PP}_{input} + PP_{r,US} - Q_r \frac{\mathrm{PP}_r}{V_r}$$

c) Daily fluxes and mean daily concentrations of TDP and PP

Time series of total daily fluxes of TDP and PP leaving the reach are obtained by integrating the instantaneous fluxes with respect to time, starting each day with initial conditions of zero (Equation 41). These total daily fluxes are then used in the calculation of daily mean TDP and PP concentrations (Equation 42), converted from units of kg mm^{-1} to mg l^{-1} for comparison with observations.

Equation 41: Rate of change of daily flux of dissolved and particulate P from the stream reach (kg day^{-1})

$$\frac{d\mathrm{TDP}_{r,df}}{dt} = Q_r \frac{\mathrm{TDP}_r}{V_r};\ \frac{d\mathrm{PP}_{r,df}}{dt} = Q_r \frac{\mathrm{PP}_r}{V_r}$$

Equation 42: Daily mean concentrations of TDP and PP in the stream reach, $TDP_{r,conc}$ and $PP_{r,conc}$ (mg l^{-1})

$$\mathrm{TDP}_{r,conc} = \frac{\mathrm{TDP}_{r,df}}{Q_{r,av}} \frac{1}{A_{SC}};\ \mathrm{PP}_{r,conc} = \frac{\mathrm{PP}_{r,df}}{Q_{r,av}} \frac{1}{A_{SC}}$$

4.4 Summary of equations, initial conditions and input parameters

Table 9 summarises the 19 ODEs which are solved simultaneously for each reach in the catchment. For the first time step initial conditions must be supplied for each ODE. To define these, three parameters are specified by the user: in-stream flow in the top reach, total soil P content and soil water TDP concentration in the 'high P' class. If the snow module is run, initial snow depth is also required. All other initial conditions are derived from these parameters or using simple assumptions – details are provided in Table 9. Initial instream masses of SS, PP and TDP are set to 0, so a burn-in period is required (the length of burn-in depends on the residence time in the reach, but should be of the order of days – weeks).

ODE	**Equation**	**Initial conditions (first time step)**
dV_s/dt For agricultural & semi-natural	Equation 6	$V_{s,0} = V_{FC}$
dQ_s/dt For agricultural & semi-natural	Equation 10	$Q^i_{s,0} = \frac{V_s^i - V_{FC}}{T_s^i\left(1+e^{V_{FC}-V_s^i}\right)}$; where superscript i denotes the land class
dV_g/dt	Equation 11	$V_{g,0} = Q_{g,0}\, T_g$
dQ_g/dt	Equation 13	$Q_{g,0} = \beta\, Q_{s,0}$
dV_r/dt	Equation 14	$V_{r,0} = Q_{r,0}\, T_{r,0}$; where $T_{r,0} = \frac{L_{reach}}{8.64\times10^4 a Q_{r0}^{0.42}}$
dQ_r/dt	Equation 17	Reach 1: Input parameter $Q_{r0,init}$ (units converted to mm day^{-1} in model) Downstream reaches: $Q_{r,0} = Q_{r,av}$ from the upstream reach for day 1
dQ_{r_av}/dt	Equation 18	0.0
dM_{sus}/dt	Equation 19	0.0
$dM_{sus,out}/dt$	Equation 23	0.0
dP_{labile}/dt For arable & newly-converted	Equation 33	Equation 31
$dTDP_s/dt$ For agricultural & new semi-natural	Equation 34	$TDP_{s,0} = A_{SC}\, EPC_{0,user}\, V_s$
$dTDP_r/dt$	Equation 38	0.0
$dTDP_{r,out}/dt$	Equation 41	0.0
dPP_r/dt	Equation 40	0.0
$dPP_{r,out}/dt$	Equation 41	0.0

Table 9: Ordinary differential equations (ODEs) solved within the model and information on how the initial conditions are defined for the first time step.

The model requires a number of parameters which should be calculated for example using a GIS (Table 10). These parameter values are likely to be well-constrained, and therefore generally will not form part of any calibration procedure (although if they are uncertain they could be included in an uncertainty analysis).

Param	Units	Description
A_{SC}	km^2	Sub-catchment area
f_{Ar}	none	Proportion of arable or other high soil P, high erodibility land (excluding newly-converted from SN)
f_{IG}	none	Proportion of improved grassland or other high soil P, moderate erodibility land (excluding newly-converted from SN)
f_S	none	Proportion of semi-natural and other low soil P land (excluding newly-converted from agricultural)
f_{NC_Ar}	none	Proportion of newly-converted arable land (from SN)
f_{NC_IG}	none	Proportion of newly-converted improved grassland (from SN)
f_{NC_S}	none	Proportion of newly-converted semi-natural land (from agricultural)
f_{spr}	none	Proportion spring-sown crops make to total arable land area (assume rest is autumn-sown)
S_{Ar}	degrees	Mean slope of arable land in the sub-catchment
S_{IG}	degrees	Mean slope of improved grassland in the sub-catchment
S_{SN}	degrees	Mean slope of semi-natural land in the sub-catchment
L_{reach}	m	Reach length
S_{reach}	degrees	Reach slope (ideally length-weighted)

Table 10: General model parameters derived using a GIS, whose values will usually be kept constant during model calibration.

The remaining model parameters are likely to be less well constrained, and are summarised in Table 11, together with suggested default values, recommended ranges, and potential data sources that could be used to inform the parameter values. An additional model parameter, $C_{measures}$, is not a calibration parameter and is only given a value when the user wishes to investigate the impact of sediment reduction measures on in-stream SS and PP concentrations or loads. There are 23 parameters in Table 11, 24-27 when spatial variability between land use classes is taken into account. Only one of these varies by sub-catchment or reach (effluent inputs), and so model complexity will not increase substantially in larger systems compared to smaller ones. At least 8 of these model parameters are optional (before taking spatial variability into account; Table 11), so in a given setup the actual number of parameters requiring calibration may be much less than 27. Even in the most complex setup in which all 27 parameters are required, an algorithm could potentially search the entire parameter space so that all could be auto-calibrated, provided the user has a full suite of water quality observations for calibration and testing (i.e. observed discharge, suspended sediment, dissolved and particulate P concentrations under the full range of flow conditions). In addition, plausible ranges for the majority of parameters may be based on measured data or data derived from literature reviews. Only four or five parameters must be determined purely through calibration (Table 11). One of these unmeasurable parameters relates to the suspended sediment simulation (E_M); the rest are hydrology parameters.

Table 11: SimplyP model parameters, including default values, recommended ranges and possible data sources. 'Spatial' column describes whether the parameter varies spatially by land use (LU), in which case by which LU type (A: agricultural, S: seminatural, Ar: arable, IG: improved grassland), or sub-catchment/reach (SC/R). Parameters likely to be key in most settings are marked with an asterisk. Many of those without an asterisk are optional. Q is discharge

Type	Param	Units	Description	Spatial	Tarland	Default	Min	Max	Data sources
Snow	$D_{snow,0}$	mm	Initial snow depth	–	0	0	0	10000	Meteorological records
	f_{DDSM}	mm dd°C^{-1}	Degree-day factor for snow melt	–	2.74	2.74	1.6	6	Literature, e.g. USDA (2004)
Hydrology	*T_s	days	Soil water time constant	LU (A, S)	A: 2 S: 10	A: 1 S: 10	> 0	30	*Calibration*
	f_{quick}	none	Proportion of precipitation routed to quick flow	–	0.02	0.02	0	0.2	*Calibration*
	alpha	none	PET reduction factor	–	1	1	0.4	1.2	Literature, e.g. Allen et al. (1998)
	*FC	mm	Soil field capacity	–	290	300	100	400	Soils database, or from soil texture using conversion charts (e.g. Appendix, Figure A1)
	*beta	none	Baseflow index	–	0.70	0.60	0	1	Local or global databases (e.g. Beck et al., 2013)
	*T_g	days	Baseflow recession constant	–	65	65	> 0	100	May be estimated from Q data using methods of Van Dijk (2010); see Beck et al. (2013) for a global analysis
	$Q_{g,min}$	mm d^{-1}	Minimum groundwater flow	–	0.4	0.0	0	2	*Calibration*
	a	m^{-2}	Gradient of stream velocity-Q relationship	–	0.5	0.5	0.1	0.8	Empirically-derived from paired velocity and Q measurements (e.g. from flow gauging)
	Q_{r0_init}	m^3 s^{-1}	Initial in-stream Q	–	1.0	1.0	> 0	N/A	Q observations
Sediment	C_{cover}	None	Vegetation cover factor (ratio of erosion rates under the land class vs bare soil)	LU (Ar, IG, S)	A: 0.2 S: 0.021 IG: 0.09	A: 0.2 S: 0.021 IG: 0.09	0	1	(R)USLE literature, e.g. Panagos et al. (2015)
	*E_M	kg mm^{-1}	Sediment input scaling factor	–	1500	1500	0	5000	*Calibration*
	*k_M	none	Sediment input non-linear coefficient	–	2.0	2.0	1.2	3	Empirical relationship between Q and SS observations or literature (e.g. Asselman, 2000)
	$d_{maxE,spr}$	none	Julian day with max erodibility; spring-sown crops	–	60	60	1	365	Local agronomic practices
	$d_{maxE,aut}$	none	Julian day with max erodibility, autumn-sown crops	–	304	304	1	365	Local agronomic practices
Dissolved P	*$P_{soilConc}$	mg kg^{-1}	Initial total soil P content	LU (A, S)	A: 1458 S: 873	A: 1458 S: 873	0-400	>3000	Soils database. Estimate from soil test P data using an empirical relationship
	*$P_{netInput}$	kg ha^{-1} yr^{-1}	Net annual P input to the soil (negative if uptake > input); S fixed at 0	LU (A)	10	10	-30	30	Fertilizer and manure application surveys, literature for P uptake, national P balance inventories (e.g. eurostat, 2013, for EU countries)
	*$EPC_{0,init}$	mg l^{-1}	Initial soil water TDP concentration on agricultural land	LU (A)	0.1	0.1	0	2	Direct measurements, literature
	*$M_{soil,m2}$	kg m^{-2}	Soil mass per m^2, important in determining the initial soil labile P mass	–	95	100	>0	800	Soils data (bulk density and depth)
	*TDP_{eff}	kg day^{-1}	Reach effluent TDP inputs	SC/R	0.1	0	0	N/A	Water company/environment protection agency data
	*TDP_g	mg l^{-1}	Groundwater TDP concentration	–	0.02	0	0	2	Direct measurements or literature
PP	*E_{PP}	none	PP enrichment factor	–	1.6	1	1	6	Direct measurements or literature (e.g. Sharpley, 1980)

4.5 Numerical methods

The model equations summarised in Section 4.4 must be solved numerically. Simply put, this involves providing initial conditions describing the state of the system, and then using the model equations to project forward in time to predict the new state of the system at the end of the time step. This then becomes the initial condition for the next time step, and the process is repeated. This process of numerical approximation introduces errors, and minimizing these errors by formulating and solving the governing model equations in a robust way is an important part of the model development process. Indeed, Clark and Kavetski (2010) suggest that in some cases numerical errors may be larger than model structural errors. Additional benefits of a robust numerical model include a smoother objective function relating model input parameters and model output (Kavetski et al., 2006a), which may reduce model calibration difficulties by allowing powerful classical parameter analysis techniques for optimisation and uncertainty analysis to be used. Kavetski et al. (2006b) argue that many of the difficulties in hydrological modelling over the last two decades, which have prompted the development of complex parameter estimation tools, are in fact due to (1) discontinuous model structures, where sharp internal thresholds introduce non-smoothness into the objective function, and to (2) poor choice of ODE solver. An attempt was made to avoid the first of these issues by avoiding thresholds in the model equations (e.g. using continuous functions rather than logic checks in equations in Section 4.1.2b). The final part of the model-building process was then to choose an appropriate ODE solver. Three factors were taken into account: (1) whether the solver is appropriate for stiff or non-stiff equations, related to the time-stepping scheme used (see below); (2) popularity, and (3) availability.

Differential equations may be categorised as stiff or non-stiff. Generally speaking, stiff equations include some terms which can lead to rapid variation in the solution, which means that certain numerical methods for solving them are unstable unless the step size taken is excessively small in relation to the smoothness of the exact solution. Time-stepping in this context relates to the sub-steps the model time step is broken down into by the solver. Most of the classical numerical methods for solving ODEs are only suitable for non-stiff ODEs (e.g. the simple Euler method, the 4^{th} order and various adaptive Runge-Kutta methods and the multi-step Adams' method). If applied to stiff systems, these methods are likely to be inaccurate or prohibitively slow. Many ODE systems are stiff in practice, and a wide range of off-the-shelf ODE solvers are available which are able to adapt their time-stepping routine and fluctuate between using stiff or non-stiff solvers. It is therefore surprising that many catchment models continue to use simple, often unsuitable solvers (Kavetski and Clark, 2011). Here, the LSODA solver was chosen, taken from the FORTRAN ODPEPACK library (Hindmarsh, 1983). LSODA starts using a non-stiff method (an Adams predictor-corrector method) and dynamically monitors the data, if necessary switching to a stiff method (the multi-step Backward Differentiation Formula method). LSODA is both widely-used and easy to implement using the SciPy.integrate module's odeint function.

The solver's error tolerance parameters affect the precision of the result, with a smaller error tolerance resulting in more time steps and greater precision but longer run times. Testing showed an approximate log relationship between run times and the relative error tolerance parameter (*rtol*), with a decrease in run times of around 70% for an increase in *rtol* from the default of 1×10^{-8} to 0.05. *rtol* was set to 0.01, to optimise the trade-off between decrease in run time and loss in accuracy. The maximum number of within-timestep function evaluations was set to 5000, to prevent the solver reaching the maximum threshold before finding a solution within the required error tolerance, which could introduce errors.

5. Future model development priorities

A number of potential areas for model improvement are highlighted throughout Section 4 and are summarised in Table 12. Most of these suggestions involve an increase in model complexity, and before being adopted any increase in complexity needs to be justified by demonstrating a substantial increase in model performance, preferably within a statistical model comparison framework. To help prioritise areas for model improvement from within this list (or indeed to highlight other areas), the model needs to be tested in

a range of contrasting catchments, including catchments where internal processes and fluxes have been measured.

Additional general recommendations for model improvement include:

- On a practical level, the model is currently slow to run compared to professionally-coded models such as INCA-P. This may be because of the choice of ODE solver, which is sophisticated compared to the solvers employed by most water quality models, or because the model is coded in Python rather than a faster, lower-level language such as C^{++}. Other solvers should be investigated for speed.
- At present, there is no flexibility in the model in terms of the number of land use classes, which are fixed at two (for dissolved P processes) or three (for sediment and PP). This reduces the versatility of the model, and future development to increase flexibility in this regard could widen the appeal of the model. However, it would also require a re-conceptualisation of the soil P equations.
- As pointed out by Adams et al. (2016), new monitoring techniques mean that high frequency P concentration measurements are now available, e.g. at 30 minute resolution, and yet many popular water quality models are only able to simulate at a daily resolution. A simple change to the model described here would be to allow the user to specify the time step required.
- Improved representation of critical source areas, by taking spatial variability in hydrology, sediment and phosphorus sources, mobilisation processes and transport/delivery pathways into account in a fuller way.

Hydrology and snow:

- Add in a PET calculation, so that the model can be run using just precipitation and temperature as inputs.
- Refinements needed to the simple degree-day approach to simulating snow melt in areas with higher snowfall?
- Include a more detailed representation of temperature variation throughout a day in the snow melt calculation.
- Is model performance improved by adding a parameter to define a lower threshold for precipitation inputs, below which quick flow is zero?
- Should quick flow be varied by land class? If so, is there still a need for different soil water time constants in the land classes?
- Add an upper limit to the soil water volume (at the saturation capacity); water above this is routed to quick flow.
- Replace the minimum groundwater flow threshold parameter with a more process-based representation. E.g. factor in percolation from the soil when soil water level drops below field capacity, but at a reduced rate.

Sediment:

- Should the sediment equations be amended to attempt to track the store of sediment in the near-channel sources, to be able to simulate source-exhaustion?
- Soil erodibility may also be affected by soil wetness, which could be factored in to Equation 21.
- The slope factor in Equation 21 could be altered to be more representative of potential sediment source areas. E.g. the average slope of land within a certain distance of the watercourse.
- An additional factor could be introduced to Equation 21 to represent connectivity between sediment source areas and the watercourse.
- The C_{cover} factor for semi-natural land could be extended to incorporate knowledge on the factors which affect erodibility, such as grazing, burning and felling.
- More testing is required to determine whether the additional complexity of a dynamic C_{cover} factor is warranted, and if so whether the adopted approach is suitable.
- Under what circumstances should sediment deposition to the stream bed be taken into account, and how could this relatively complex process be represented in a simple way?
- Can reach sediment (and PP) inputs be split into inputs from the land versus bank erosion in a simple way? Work on sediment fingerprinting may help.
- Should a distinction be made between allochthonous & autochthonous in-stream sediment and PP?

Phosphorus:

- Add in an option for the net P input parameter to be dynamic, for example as a user-input time series. In addition, a link between soil P content and net P uptake would improve simulations of the longer term soil P dynamics (though is likely to require soil test P to be simulated).
- Geochemical models or lab experiments could inform the adsorption coefficient in Equation 27, e.g. by providing a range of parameters for a suite of soil types with a range of P sorption capacities.
- Add the ability to input soil P as soil test P rather than total soil P. This could be a user-specified linear relationship, but a more advanced geochemical representation may be required for meaningful results to be obtained.
- A dynamic PP enrichment factor could replace the constant, for example linked to discharge.
- To simulate legacy groundwater TDP, a simple link is needed between soil water and groundwater TDP concentration, predictable using readily-measurable groundwater properties.
- Add in an option for effluent inputs to be read in from a time series, rather than being constant.
- When/where is it necessary to explicitly account for in-stream TDP sinks (e.g. adsorption or biological uptake of sewage effluent P)? A simple decay factor may be sufficient.
- When/where should P desorption from the stream bed be simulated? How should this be done?
- For reaches with longer residence times, a link may be needed between in-stream PP and TDP.
- Sewage PP inputs could be added.
- More process-based representation of septic tank inputs.
- Ability to predict SRP concentrations, either using a simple linear regression between TDP and SRP, or by taking into account the TDP:SRP ratio of agricultural versus sewage effluent P inputs.

Table 12: Examples of areas for future model development.

References

Allen, R., Pereira, L., Raes, D., and Smith, M. (1998). "Crop evapotranspiration – guidelines for computing crop water requirements. FAO irrigation and drainage paper 56."

Asselman, N. E. M. (2000). Fitting and interpretation of sediment rating curves. *Journal of Hydrology* **234**, 228-248.

Bagnold, R. (1966). An approach to the sediment transport problem. *General Physics Geological Survey, Prof. paper*.

Beck, H. E., Dijk, A. I., Miralles, D. G., Jeu, R. A., McVicar, T. R., and Schellekens, J. (2013). Global patterns in base flow index and recession based on streamflow observations from 3394 catchments. *Water Resources Research* **49**, 7843-7863.

Bowes, M. J., House, W. A., Hodgkinson, R. A., and Leach, D. V. (2005). Phosphorus–discharge hysteresis during storm events along a river catchment: the River Swale, UK. *Water Research* **39**, 751-762.

Chapra, S. C. (2008). "Surface water-quality modeling," Waveland press.

Clark, M. P., and Kavetski, D. (2010). Ancient numerical daemons of conceptual hydrological modeling: 1. Fidelity and efficiency of time stepping schemes. *Water Resources Research* **46**, W10510.

Colby, B. (1956). "Relationship of sediment discharge to streamflow," Rep. No. 2331-1258. US Dept. of the Interior, Geological Survey, Water Resources Division.

Croke, B. F., Andrews, F., Jakeman, A. J., Cuddy, S. M., and Luddy, A. (2006). IHACRES Classic Plus: a redesign of the IHACRES rainfall-runoff model. *Environmental Modelling & Software* **21**, 426-427.

Dari, B., Nair, V., Colee, J., Harris, W., and Mylavarapu, R. (2015). Estimation of Isotherm Parameters: A Simple and Cost-effective Procedure. *Frontiers in Environmental Science* **3**.

Dean, S., Freer, J., Beven, K., Wade, A. J., and Butterfield, D. (2009). Uncertainty assessment of a process-based integrated catchment model of phosphorus. *Stochastic environmental research and risk assessment* **23**, 991-1010.

Domagalski, J. L., and Johnson, H. M. (2011). Subsurface transport of orthophosphate in five agricultural watersheds, USA. *Journal of Hydrology* **409**, 157-171.

eurostat (2013). Agri-environmental indicator fact sheet - risk of pollution by phosphorus. *In* "European Union (EU) agri-environmental indicator fact sheets".

Fenicia, F., Kavetski, D., and Savenije, H. H. G. (2011). Elements of a flexible approach for conceptual hydrological modeling: 1. Motivation and theoretical development. *Water Resources Research* **47**, n/a-n/a.

Fenicia, F., Savenije, H. H. G., Matgen, P., and Pfister, L. (2006). Is the groundwater reservoir linear? Learning from data in hydrological modelling. *Hydrol. Earth Syst. Sci.* **10**, 139-150.

Futter, M. N., Erlandsson, M. A., Butterfield, D., Whitehead, P. G., Oni, S. K., and Wade, A. J. (2014). PERSiST: a flexible rainfall-runoff modelling toolkit for use with the INCA family of models. *Hydrol. Earth Syst. Sci.* **18**, 855-873.

Gan, R., and Luo, Y. (2013). Using the nonlinear aquifer storage–discharge relationship to simulate the base flow of glacier- and snowmelt-dominated basins in northwest China. *Hydrol. Earth Syst. Sci.* **17**, 3577-3586.

Hindmarsh, A. C. (1983). ODEPACK, A Systematized Collection of ODE Solvers, RS Stepleman et al.(eds.), North-Holland, Amsterdam,(vol. 1 of), pp. 55-64. *IMACS transactions on scientific computation* **1**, 55-64.

Holman, I. P., Whelan, M. J., Howden, N. J. K., Bellamy, P. H., Willby, N. J., Rivas-Casado, M., and McConvey, P. (2008). Phosphorus in groundwater—an overlooked contributor to eutrophication? *Hydrological Processes* **22**, 5121-5127.

House, W. A. (2003). Geochemical cycling of phosphorus in rivers. *Applied Geochemistry* **18**, 739-748.

Jackson-Blake, L. A., Dunn, S. M., Helliwell, R. C., Skeffington, R. A., Stutter, M. I., and Wade, A. J. (2015). How well can we model stream phosphorus concentrations in agricultural catchments? *Environmental Modelling & Software* **64**, 31-46.

Jackson-Blake, L. A., and Starrfelt, J. (2015). Do higher data frequency and Bayesian auto-calibration lead to better model calibration? Insights from an application of INCA-P, a process-based river phosphorus model. *Journal of Hydrology* **527**, 641-655.

Jarvie, H. P., Sharpley, A. N., Spears, B., Buda, A. R., May, L., and Kleinman, P. J. A. (2013a). Water Quality Remediation Faces Unprecedented Challenges from "Legacy Phosphorus". *Environmental Science & Technology* **47**, 8997-8998.

Jarvie, H. P., Sharpley, A. N., Withers, P. J. A., Scott, J. T., Haggard, B. E., and Neal, C. (2013b). Phosphorus Mitigation to Control River Eutrophication: Murky Waters, Inconvenient Truths, and "Postnormal" Science. *J. Environ. Qual.* **42**, 295-304.

Jordan-Meille, L., Rubæk, G. H., Ehlert, P. A. I., Genot, V., Hofman, G., Goulding, K., Recknagel, J., Provolo, G., and Barraclough, P. (2012). An overview of fertilizer-P recommendations in Europe: soil testing, calibration and fertilizer recommendations. *Soil Use and Management* **28**, 419-435.

Kavetski, D., and Clark, M. P. (2011). Numerical troubles in conceptual hydrology: Approximations, absurdities and impact on hypothesis testing. *Hydrological Processes* **25**, 661-670.

Kavetski, D., Kuczera, G., and Franks, S. W. (2006a). Calibration of conceptual hydrological models revisited: 1. Overcoming numerical artefacts. *Journal of Hydrology* **320**, 173-186.

Kavetski, D., Kuczera, G., and Franks, S. W. (2006b). Calibration of conceptual hydrological models revisited: 2. Improving optimisation and analysis. *Journal of Hydrology* **320**, 187-201.

Kinnell, P. I. A. (2010). Event soil loss, runoff and the Universal Soil Loss Equation family of models: A review. *Journal of Hydrology* **385**, 384-397.

Kleinman, P., Sharpley, A., Buda, A., McDowell, R., and Allen, A. (2011). Soil controls of phosphorus in runoff: Management barriers and opportunities. *Canadian Journal of Soil Science* **91**, 329-338.

Lefrançois, J., Grimaldi, C., Gascuel-Odoux, C., and Gilliet, N. (2007). Suspended sediment and discharge relationships to identify bank degradation as a main sediment source on small agricultural catchments. *Hydrological Processes* **21**, 2923-2933.

Leopold, L. B., and Maddock Jr, T. (1953). "The hydraulic geometry of stream channels and some physiographic implications," Rep. No. 2330-7102.

Luo, Y., Arnold, J., Allen, P., and Chen, X. (2012). Baseflow simulation using SWAT model in an inland river basin in Tianshan Mountains, Northwest China. *Hydrol. Earth Syst. Sci.* **16**, 1259-1267.

McCray, J. E., Kirkland, S. L., Siegrist, R. L., and Thyne, G. D. (2005). Model Parameters for Simulating Fate and Transport of On-Site Wastewater Nutrients. *Ground Water* **43**, 628-639.

Menzel, R. (1980). Enrichment ratios for water quality modeling. *CREAMS: A Field-Scale Model for Chemicals, Runoff, and Erosion from Agricultural Management Systems Conservation Research Report Number 26, May, 1980. p 486-492, 1 Fig, 2 Tab, 11 Ref.*

Merritt, W. S., Letcher, R. A., and Jakeman, A. J. (2003). A review of erosion and sediment transport models. *Environmental Modelling & Software* **18**, 761-799.

Neal, C., Jarvie, H. P., Neal, M., Love, A. J., Hill, L., and Wickham, H. (2005). Water quality of treated sewage effluent in a rural area of the upper Thames Basin, southern England, and the impacts of such effluents on riverine phosphorus concentrations. *Journal of Hydrology* **304**, 103-117.

Oeurng, C., Sauvage, S., and Sánchez-Pérez, J.-M. (2010). Dynamics of suspended sediment transport and yield in a large agricultural catchment, southwest France. *Earth Surface Processes and Landforms* **35**, 1289-1301.

Panagos, P., Borrelli, P., Meusburger, K., Alewell, C., Lugato, E., and Montanarella, L. (2015). Estimating the soil erosion cover-management factor at the European scale. *Land Use Policy* **48**, 38-50.

Radcliffe, D. E., and Cabrera, M. L. (2006). "Modeling phosphorus in the environment," CRC Press.

Ratliff, L. F., Ritchie, J. T., and Cassel, D. K. (1983). Field-Measured Limits of Soil Water Availability as Related to Laboratory-Measured Properties1. *Soil Science Society of America Journal* **47**.

Renard, K. G., Foster, G. R., Weesies, G. A., and Porter, J. P. (1991). RUSLE: Revised universal soil loss equation. *Journal of soil and Water Conservation* **46**, 30-33.

Sample, J. (2015). Statistics notes for environmental modelling. GitHub.

Sharpley, A., Jarvie, H. P., Buda, A., May, L., Spears, B., and Kleinman, P. (2013). Phosphorus Legacy: Overcoming the Effects of Past Management Practices to Mitigate Future Water Quality Impairment. *J. Environ. Qual.* **42**, 1308-1326.

Sharpley, A. N. (1980). The Enrichment of Soil Phosphorus in Runoff Sediments1. *J. Environ. Qual.* **9**, 521-526.

Starrfelt, J., and Kaste, O. (2014). Bayesian uncertainty assessment of a semi-distributed integrated catchment model of phosphorus transport. *Environmental Science: Processes & Impacts* **16**, 1578-1587.

Stollenwerk, K. G. (1996). Simulation of phosphate transport in sewage-contaminated groundwater, Cape Cod, Massachusetts. *Applied Geochemistry* **11**, 317-324.

Stutter, M. I., Demars, B. O. L., and Langan, S. J. (2010). River phosphorus cycling: Separating biotic and abiotic uptake during short-term changes in sewage effluent loading. *Water Research* **44**, 4425-4436.

Stutter, M. I., Langan, S. J., Lumsdon, D. G., and Clark, L. M. (2009). Multi-element signatures of stream sediments and sources under moderate to low flow conditions. *Applied Geochemistry* **24**, 800-809.

Stutter, M. I., and Lumsdon, D. G. (2008). Interactions of land use and dynamic river conditions on sorption equilibria between benthic sediments and river soluble reactive phosphorus concentrations. *Water Research* **42**, 4249-4260.

Trimble, S. W. (2010). Streams, valleys and floodplains in the sediment cascade. *Sediment Cascades: An Integrated Approach*, 307-343.

Twarakavi, N. K. C., Sakai, M., and Šimůnek, J. (2009). An objective analysis of the dynamic nature of field capacity. *Water Resources Research* **45**, n/a-n/a.

USDA (2004). "National Enginnering Handbook, Part 630 - Hydrology, Chapter 11 (Snowmelt)." United States Department of Agriculture, Natural Resources Conservation Service.

Van Dijk, A. (2010). Climate and terrain factors explaining streamflow response and recession in Australian catchments. *Hydrology and Earth System Sciences* **14**, 159-169.

Wischmeier, W. C., and Smith, D. D. (1965). "Predicting rainfall-erosion losses from cropland east of the Rocky Mountains.," US Department of Agriculture (USDA), Washington DC.

Wischmeier, W. C., and Smith, D. D. (1978). "Predicting rainfall erosion losses - a guide to conservation planning," US Department of Agriculture (USDA), Washington DC.

Withers, P. J. A., and Jarvie, H. P. (2008). Delivery and cycling of phosphorus in rivers: A review. *Science of the Total Environment* **400**, 379-395.

Wittenberg, H. (1999). Baseflow recession and recharge as nonlinear storage processes. *Hydrological Processes* **13**, 715-726.

Wolman, M., Miller, J., and Leopold, L. (1964). Fluvial processes in geomorphology. *San Francisco*.

Appendix A: Data to help with model parameterisation

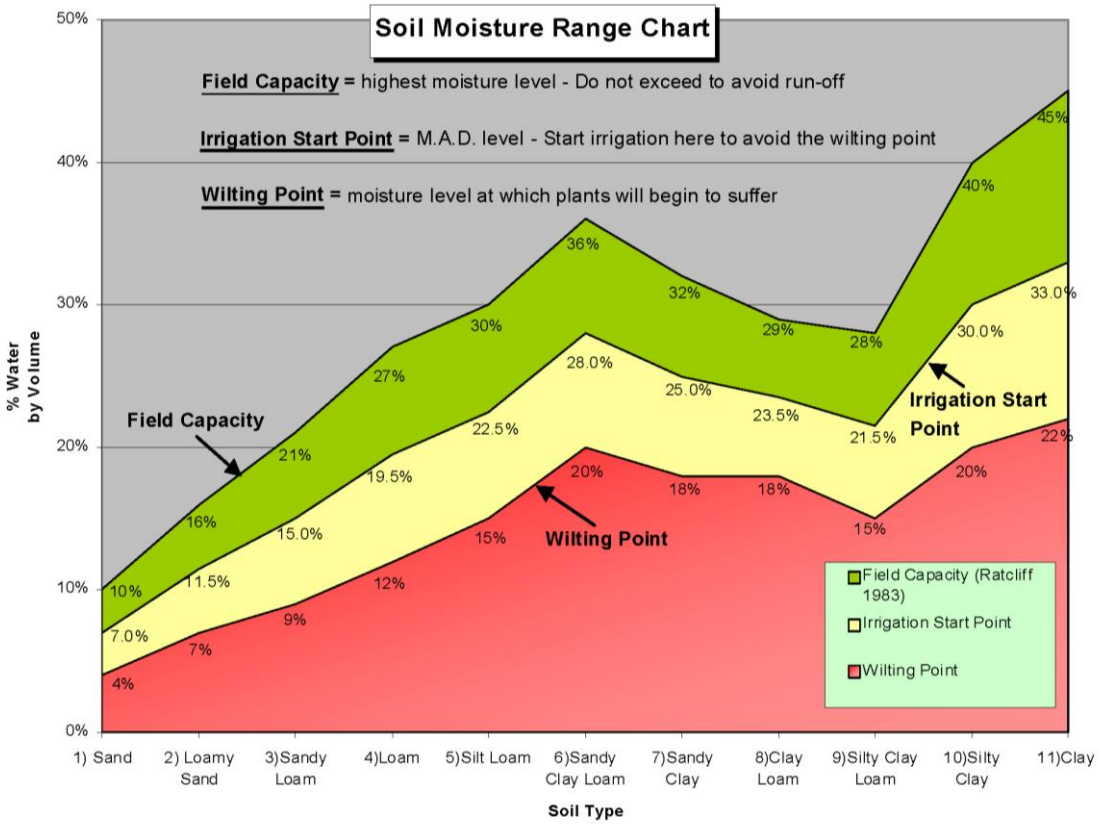

Figure A1: Chart for estimating field capacity based on soil texture, if only the latter is known.
Source: ftp://ftp.dynamax.com/turf_irrigation/Soil%20Moisture%20Range%20Chart.pdf

Crop type	C-factor
Common wheat and spelt	0.2
Durum wheat	0.2
Rye	0.2
Barley	0.21
Grain maize – corn	0.38
Rice	0.15
Dried pulses (legumes) and protein crop	0.32
Potatoes	0.34
Sugar beet	0.34
Oilseeds	0.28
Rape and turnip rape	0.3
Sunflower seed	0.32
Linseed	0.25
Soya	0.28
Cotton seed	0.5
Tobacco	0.49
Fallow land	0.5

Table A1: USLE cover factors for typical European crops (Panagos et al., 2015)

Group	Detailed class	Description	C-factor	UK mean
Permanent crops	Vineyards	Vineyards	0.15–0.45	
	Fruit trees & berry plantations	Fruit trees or shrubs: single/mixed fruit species, fruit trees with permanently grassed surfaces	0.1–0.3	
	Olive groves	Olive trees	0.1–0.3	
Pastures	Pastures	Dense graminoid grass cover of floral composition, not under a rotation system. Mainly used for grazing.	0.05–0.15	0.0867
Heterogeneous agricultural areas	Annual crops associated with permanent crops	Non-permanent crops (arable land or pasture) associated with permanent crops (<25% non-associated crops)	0.07–0.35	
	Complex cultivation patterns	Small parcels of annual crops, pasture and/or permanent crops (each occupy less than 75% of the total area)	0.07–0.2	0.1201
	Principally agriculture, significant areas of natural vegetation	Principally agricultural, with natural areas (agricultural land occupies 25 to 75% of the area)	0.05–0.2	0.1068
	Agro-forestry	Annual crops or grazing land under forested cover	0.03–0.13	
Forests	Broad-leaved, coniferous and mixed forest	Principally trees including shrub and bush understories	0.0001–0.003	0.0011
Scrub and/or herbaceous vegetation	Natural grasslands	Low productivity grassland, often on rough and uneven ground	0.01–0.08	0.0319
	Moors and heathland	Low and closed cover dominated by bushes, shrubs and herbaceous plants	0.01–0.1	
	Sclerophyllous vegetation	Bushy sclerophyllous vegetation, including maquis (dense, shrubby) and garrige	0.01–0.1	
	Transitional woodland-shrub	Bushy or herbaceous vegetation with scattered trees	0.003–0.05	0.0183
Open spaces with little or no vegetation	Beaches, dune, sands	Beaches, dunes and expanses of sand/pebbles. Coastal or continental	0	
	Bare rocks	Scree, cliffs, rocks and outcrops	0	
	Sparsely vegetated areas	Includes steppes, tundra, badlands. Scattered high-altitude vegetation	0.1–0.45	0.1825
	Burnt areas	Areas affected by recent fires, still mainly black	0.1–0.55	
	Glaciers and perpetual snow	Land covered by glaciers or permanent snowfields	0	

Table A2: USLE cover factors collated for European land cover classes (Panagos et al., 2015)